GULF STATES UTILITIES COMPANY
POST OFFICE BOX 2951 • BEAUMONT, TEXAS 77704
AREA CODE 409 838-6631

July 31, 1986
RBG- 24,131
File No. G9.5

Mr. H.R. Denton, Director
Office of Nuclear Reactor Regulation
U.S. Nuclear Regulatory Commission
Washington, D. C. 20555

Dear Mr. Denton:

River Bend Station - Unit 1
Docket No. 50-458

Gulf States Utilities (GSU) January 23, 1985 letter (RBG-19,972) transmitted GSU's final updated response to containment issues. Your review and remaining open items are documented in Supplement No. 2 - Appendix K of the River Bend Station Safety Evaluation Report (NUREG-0989), a June 25, 1985 letter from H. R. Denton to W.J. Cahill requesting additional information, and NPF-47 License Condition 2.C.(5). The enclosure to this letter is GSU's response to these open Mark III related issues.

Enclosed are revisions to action plans 2, 5, 6 and 8. For your convenience in review the entire action plan has been included. The changes which incorporate responses to your questions are indicated with change bars. You should consider the previous action plans to be superceded by the enclosed action plans.

Prior to using the RHR System in the steam condensing mode, GSU will have received the written approval of the staff and GSU will have incorporated into the plant emergency operating procedures restrictions not to allow operation of the RHR System in the steam condensing mode following a LOCA or until the peak local and bulk suppression pool temperaures have been reduced below 130˜F.

If you require any clarification regarding the enclosure to this letter, please do not hesitate to contact Mr. L. A. England of my staff.

Sincerely,

J. E. Booker

J. E. Booker
Manager-Engineering,
Nuclear Fuels & Licensing
River Bend Nuclear Group

JEB/lp

Enclosure

A001
1/1

Action Plan 2

I. Issues Addressed - Generic/Plant Specific

1.3 Additional submerged structure loads may be applied to submerged structures near local encroachments.

II. Program for Resolution

1. The results obtained from the two-dimensional analyses completed as part of the activities for Action Plan 1 will be used to define changes in fluid velocities in the suppression pool which are created by local encroachments. Supporting arguments to verify that the results from two-dimensional analyses will be bounding with respect to velocity changes in the suppression pool will be provided.

2. The new pool velocity profiles will be used to calculate revised submerged structure loads using the existing or modified submerged load definition models.

3. The newly defined submerged structure loads will be compared to the loads which were used as a design basis for equipment and structures in the River Bend Station suppression pool.

III. Status*

Items 1, 2, and 3 are complete and the results are included in this submittal.

IV. Final Program Results*

Item 1

Additional loadings may be applied to both submerged structures and the pool boundary due to the effect of local encroachments.

Due to similarities in pool encroachments between RBS and GGNS as indicated in Table 1 of Action Plan 1, Item 6a, the results of GGNS analyses are applicable to RBS.

Pool Boundary Loads

The present load definition specifies the pool swell boundary load on the drywell wall to be the peak drywell pressure. Even with encroachments, this limit will not be affected.

The pool boundary load definition on the containment wall is 10 psid, based on PSTF full scale test data. An evaluation was performed to address the concern that the encroachment may increase the bubble pressure and cause the bubble to be translated closer to the containment wall, which could result in increased loading.

Pressure on the containment wall is a direct output of the SOLAV01 code. In the full scale PSTF geometry, the containment wall is located 19 ft from the vent exit as opposed to 20.5 ft for RBS. Since the River Bend pool is wider, the 10 psid design load is extremely conservative. The base case for evaluating the potential increase in pool boundary loads on the containment wall was established as the GGNS geometry with a 19-ft pool width. The pressure loading curve on the containment wall was calculated and then normalized so that the peak pressure corresponded to the design pressure of 10 psid. The pressure loading curve was then recalculated for the GGNS encroached case, and again normalized to the design pressure. A comparison of the base case and the design base case is presented in Figure 2-1.

The encroachment causes the wall pressure to increase by approximately 15 percent. This is, of course, only a local loading increase in the vicinity of the encroachment. This increase poses no concern from a design standpoint because the loading is of sufficient duration (0.5 sec) to be considered a static load. The 15 percent increase over the 10 psid design value is easily bounded by the 15 psid containment design pressure. Thus, encroachments do not adversely affect the boundary design loads.

The use of a 2-D code in this analysis is conservative because the encroachment is assumed to cover 360°, maximizing the wall loading. In addition, pressure gradients will exist in the areas between the projections of the vents on the containment shell. This effect will not be seen in any two-dimensional analysis, nor is it accounted for in the containment shell bubble pressure load definition.

Item 2

The results obtained from the two-dimensional SOLA analysis indicated a maximum pool swell velocity of 31 ft/sec. This is enveloped by the 50-ft/sec drag load velocity specified as the design basis in the RBS FSAR.

The RBS design basis for piping and structures above the pool surface is 60/115-psi impact load, depending on the structure shapes, followed by drag load based on 50-ft/sec pool swell velocities. For structures less than 10 ft above the pool surface, the impact pressure can be reduced using the following relation derived from equations presented in RBS FSAR Section 6.A.10.1:

$$\frac{p'}{P_{max}} = \frac{H^2}{100}\left(2.6-1.6\sqrt{\frac{H}{10}}\right)^2 \qquad [FSAR]$$

The newly defined pool swell velocities are enveloped by the design basis. For piping and structures below the pool surface, the load is bounded by the LOCA bubble drag load. The Mark III bubble encroachment series tests, along with the model-data comparison presented in the SOLAV02 computer code demonstrated that the encroached pool response during the pool swell portion of a design basis accident (DBA) in a Mark III plant will be bounded by the clean pool response.

Item 3

The pressure loadings on piping and structures above the pool surface in the vicinity of the TIP platform as a result of encroachment effects are enveloped by the 60/115-psi design impact load for piping/flat structures, respectively, as identified in GESSAR II. For piping and structures below the pool surface, the Mark III Encroachment 1/10 Linear Froude Scaled Bubble Pressure Equalization tests were conducted. High speed motion pictures and some pressure histories were obtained in clean unencroached and encroached pool areas for a series of encroachment sizes. The encroached pool velocity obtained for the encroachment series resulted in a lower velocity than for the clean pool tests. The results are attributed to bubble growth into the adjacent clean pool cell. This growth removes the driving force in the encroached region and results in a lower response. Therefore, the drag loads are considered to be bounded by the GESSAR II load specification for the clean pool case.

The SOLAV02 computer runs consisted of selected encroachment series tests selected for model-data comparison. Peak surface velocity versus elevation plots were generated. The response results, corresponding to the TIP platform encroachment design, also indicated that the clean pool response dominated.

In conclusion, the encroachment series tests and the SOLAV02 computer code predictions demonstrate that the pressure loadings produced as a result of the encroachment are bounded by the LOCA bubble loads specified as the design basis for the RBS in GESSAR II.

Based on this response, this issue is considered closed for RBS.

*This revision replaces the GSU submittal dated January 23, 1985

Figure 2-1 Effect of GGNS Encroachment on Containment Wall Boundary Load During Pool Swell

Note: A COMPARISON OF RBS AND GGNS POOL ENCROACHMENTS IS GIVEN IN TABLE 1 OF ACTION PLAN 1.

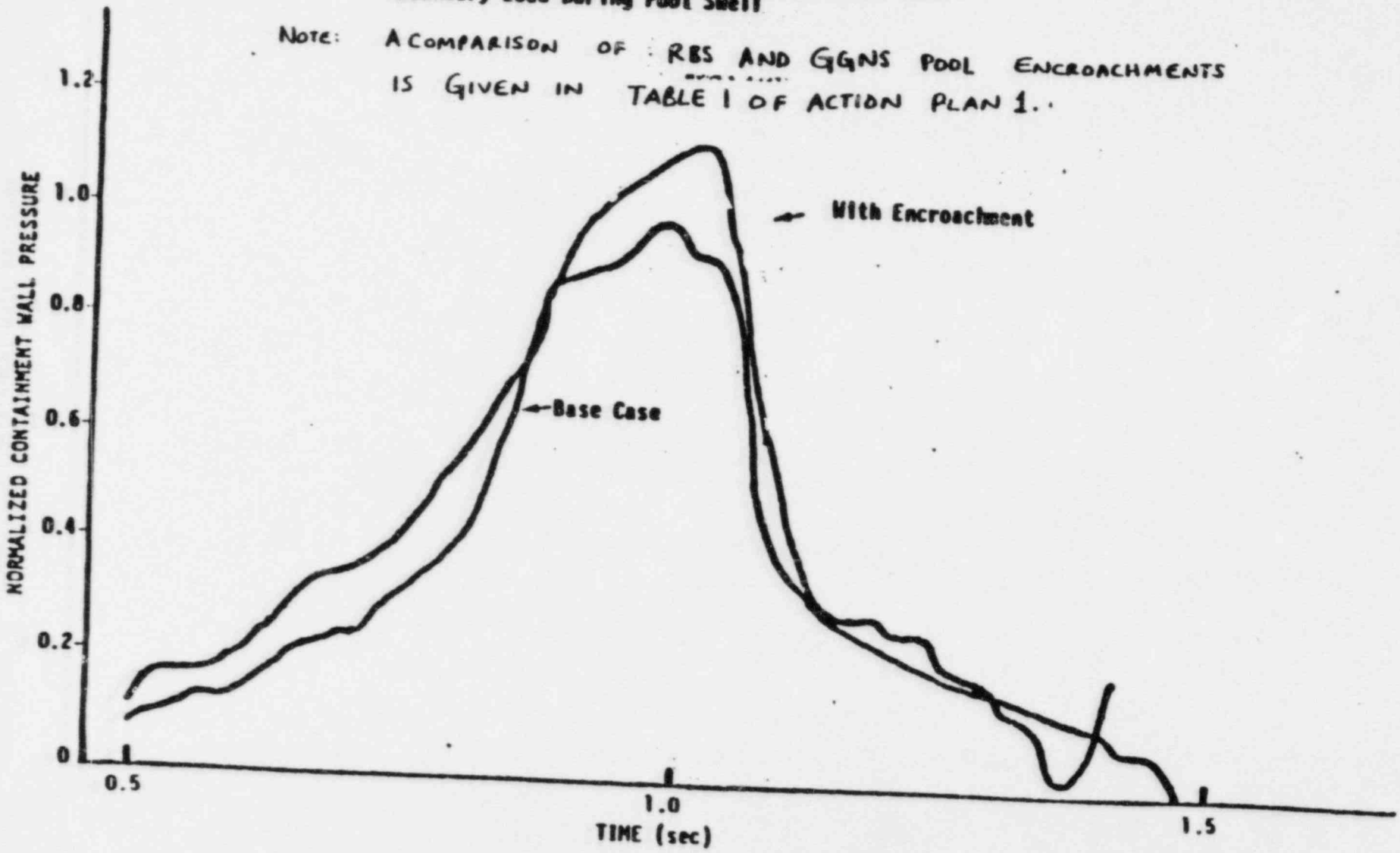

Action Plan 5 - Generic/Plant Specific

I. Issues Addressed

2.1 The annular regions between the safety relief valve lines and the drywell wall penetration sleeves may produce condensation oscillation (CO) frequencies near the drywell and containment wall structural resonance frequencies.

2.2 The potential CO and chugging loads produced through the annular area between the SRVDL and sleeve may apply unaccounted-for loads to the SRVDL. Since the SRVDL is unsupported from the quencher to the inside of the drywell wall, this may result in failure of the line.

2.3 The potential CO and chugging loads produced through the annular area between the SRVDL and sleeve may apply unaccounted-for loads to the penetration sleeve. The loads may also be produced at or near the natural frequency of the sleeve.

II. Program for Resolution

1. The existing condensation data will be reviewed to verify that no significant frequency shifts have occurred. The data will also be reviewed to confirm that the amplitudes were not closely related to acoustic effects.

2. The driving conditions for CO at the SRVDL exit will be calculated. Based on these calculations, existing test data will be used to estimate the frequency and bounding pressure amplitude of CO at the SRVDL annulus exit.

3. A wide difference between the CO frequency and structural resonances will be demonstrated. The margin between the new loads and existing loads will be quantified.

4. A detailed description of all hydrodynamic and thermal loads that are imposed on the SRVDL and SRVDL sleeve during LOCA blowdowns will be provided.

5. Ensure that thermal loads created by steam flow through the annulus have been accounted for in the design.

6. State the external pressure loads that the portion of the SRVDL enclosed by the sleeve can withstand.

7. Calculate the maximum lateral loads which could be applied to the sleeve by phenomena analogous to the Mark I and Mark II downcomer lateral loads.

III. Status*

Item 1 through 7 are complete under a previous submittal; however, some additional information has now been added to Items 1 and 7 in this submittal.

IV. Final Program Results*

Item 1

CO frequency shifts which occurred in the 1/9 area scale PSTF data are discussed in some detail in References 1 and 2. The unique size of the 1/9 scale PSTF vent caused these frequency shifts to occur. Late in the transient, the CO frequency content excited the quarter standing wave (20-24 Hz) in the PSTF pool. This caused the root mean square pressure amplitude to increase by a factor of approximately 2. The amplitude of oscillation is consequently related to acoustic effects only for the 1/9 area scale PSTF tests. Similar acoustic effects were not observed in 1/3 area scale or full scale tests.

The size of the SRVDL sleeve annulus is such that the CO frequency is much higher than the frequency which occurred in the 1/9 scale PSTF vent. The first fundamental frequency of sleeve CO is relatively close to the three-quarter standing wave in the pool. However, when standing waves have been detected in Mark III pool tests, it is only the one-quarter standing waves which have appeared. The conservative analysis performed under Item 2 of this action plan demonstrates that the factor of 2 margin exists within the design basis, which should easily encompass any acoustic effects.

The frequency in the sleeve is expected to decrease with time. Chugging should occur in the main vents effectively eliminating CO in the SRVDL-sleeve annulus before the CO frequency can approach a frequency capable of exciting the pool quarter standing wave.

* This revision replaces the GSU submittal dated January 23, 1985.

Item 1 Supplement

The NRC has expressed concern (Reference 3) that the methodology used to address this concern (Reference 4) did not account for a possible resonance between the sleeve annulus CO frequency and the sleeve acoustic frequency. To address this concern, an alternative approach for estimating the SRVDL sleeve CO load has been used, which conservatively utilizes Mark I Full Scale Test Facility (FSTF) CO data in which significant excitation of the vent acoustic modes was observed (References 5 and 6). This alternative approach shows that CO occurring in the SRVDL sleeve combined with the main vent CO gives pressures on the containment wall and drywell wall which are bounded by the pool swell and chugging loads already considered in design.

Analysis

There is substantial large scale CO data available from tests of the Mark I and Mark II vertical vents (downcomers) and the Mark III horizontal vents. Of these tests, the Mark I FSTF data (Reference 5) has the most evident excitation of vent acoustic modes. Therefore, the FSTF data were used to address the NRC concern regarding resonant amplification of the CO loads in the SRVDL sleeve.

The Mark I Load Definition Report (LDR) (Reference 6) includes a conservative definition of harmonic amplitudes for pressure oscillations in the Mark I downcomer during condensation oscillation based on the FSTF data.

These pressure oscillations were conservatively assumed to occur at the same amplitude in the Mark III SRVDL sleeve. No amplitude reduction was done to account for the differences in the exit geometry of the Mark I downcomer and the SRVDL sleeve. The Mark I downcomer discharge is a 2 foot diameter pipe while the sleeve has an annulus of approximately one foot diameter with a one inch gap. This small gap is expected to result in smaller amplitude oscillations of the steam-water interface so that the SRVDL sleeve should have much lower amplitude pressure oscillations than the Mark I downcomer. Also, no amplitude adjustment has been made to account for differences in flow conditions between the FSTF tests and the SRVDL sleeve. The Mark I tests showed that the CO pressure amplitude increased with the vent enthalpy flow (Figure 6.2.2-56 of Reference 5). The maximum enthalpy flux for the SRVDL sleeve is approximately the same as the maximum value in the FSTF tests.

The frequency range of the SRVDL sleeve CO load was determined by multiplying the Mark I LDR specified frequencies by the ratio of the FSTF vent length to the SRVDL sleeve length. This adjustment is based on the assumption that the frequencies are controlled by the acoustic response in the sleeve. The resulting ranges are shown in Table 5-1 for River Bend along with the pressure oscillation harmonic amplitudes in the sleeve and on the drywell and containment walls.

The pressure amplitudes in the sleeve given in Table 5-1 are equal to the Mark I LDR values as discussed above. The amplitudes on the drywell wall and containment wall were determined by using a spatial attenuation equal to one over the distance from the end of the sleeve. The radius of the bubble at the sleeve exit was conservatively assumed to be equal to the radius of the sleeve. Since the annulus gap will act to limit the bubble size, the actual spatial attenuation of the pressures would result in pressures on the walls which are much smaller than the values give in Table 5-1.

The amplified response spectra (ARS) values for estimated CO loads for the SRVDL sleeve and the main vent[1] are compared to ARS values for the pool swell and chugging wall loads in Figures A and B. The comparisons are based on the lowest frequency component of the SRVDL sleeve CO load. The CO loads for the two higher frequency components are less significant relative to the pool swell and chugging loads so they are not included in the comparison. This shows that the addition of the estimated SRVDL sleeve CO load to the main vent CO load results in a total CO load which is less than the chugging load on the drywell wall (Figure A) and the pool swell load on the containment wall (Figure B).

Summary

An estimate of the CO load in the SRVDL sleeve for River Bend has been made using Mark I FSTF data which includes significant excitation of the acoustic modes in the vent upstream of the discharge. This was done to address NRC concerns regarding resonant amplification resulting from coupling of the sleeve acoustic frequency and the CO frequency. The FSTF data has been conservatively applied without any amplitude reduction. The ARS of the resulting SRVDL sleeve CO load combined with the main vent CO load is lower than other DBA LOCA design loads (chugging and pool swell). Therefore it is not necessary to consider this load in design evaluations. Based on this response, this issue is considered closed for RBS.

---

1 The main vent CO ARS values are based on calculations for Grand Gulf which are representative for River Bend.

Item 2

A calculation of the steam mass flux at the SRVDL sleeve discharge during a postulated LOCA shows the CO can be expected to occur in the sleeve. The GESSAR II CO load definition pressure time-history was modified to include higher frequency components attributable to CO in the SRVDL sleeve. A comparison of amplified response spectra (ARS) of the CO pressure time-histories, which included the contribution of the sleeve with chugging and pool swell load definitions, shows that the CO loads produced in the sleeve are easily bounded by other Mark III load definitions.

SRVDL Sleeve Steam Mass Flux

The condensation mode (CO or chugging) is determined, to a large extent, by the steam mass flux. Thus, prediction of the condensation mode for discharges from the SRVDL sleeve annulus requires an estimate of the steam mass flux through the annulus. This estimate has been made by considering the SRVDL sleeves and the top row of main vents as parallel flow paths, each with a different resistance to flow. Since the sleeve annuli have a much smaller total area than the top vents, it is logical to expect that the total flow through the annuli will be small compared to the total vent flow. For parallel flow paths, the ratio of the mass fluxes can be determined from:

$$\frac{G_{sleeve}}{G_{vent}} = \sqrt{\frac{K_{vent}}{K_{sleeve}}}$$

where G is mass flux and K is a pressure loss coefficient,

$$K = P/(\rho v^2/2\ g)$$

Using the dimension of the Grand Gulf SRVDL or River Bend SRVDL sleeves

$$\frac{G_{sleeve}}{G_{vent}} \text{ is approximately equal to } 0.8$$

Since this ration is relatively close to unity, CO will occur in the sleeve during nearly the same time period of a LOCA as it occurs in the vent. To illustrate this, Figure 5-1 shows the vent and sleeve steam mass flux time-history calculated with M3CPT04 (Reference 7) for a Grand Gulf DBA. Assuming that transition from CO to chugging occurs near 10 lb/sq ft/sec, Figure 5-1 shows that generally the vent and sleeve will experience CO simultaneously.

Defining the Load on the Pool Boundary

The CO occurring in the SRVDL sleeve annuli is expected to add a high-frequency component to the basic vent CO load definition. To evaluate the effect of SRVDL sleeve CO, a modified CO pressure time-history was developed by summing the individual components of the main vent and SRVDL sleeve CO pressure histories. It was assumed that the SRVDL sleeves behave as small horizontal vents, allowing application of the Mark III CO methodology.

No data on condensation in slanted annular geometry currently exists. Therefore, a very conservative load definition has been provided to bound these geometric uncertainties. Reference 8 suggests that the wall pressure amplitude varies as the ration of vent area to pool surface area. To account for uncertainties in the condensation processes which might occur in the annular SRVDL sleeve opening, the assumption was made that the amplitude varies as the square root of the vent area to pool area ratio. This assumption increases the SRVDL sleeve CO amplitude by a factor of 4 over the result contained in Reference 8. This large factor of conservatism is used to assure that a bounding response is obtained.

For additional conservatism, the maximum local CO amplitude will be considered to act azimuthally on the entire pool boundary. Globally, the SRVDL sleeve CO effect will be smaller since there are only 20 SRVDL sleeves compared to the 45 sets of vents present. Thus, an additional factor of approximately 2 exists over the expected global response. It should be noted that RBS has only 16 SRVDL sleeves and 43 vents per row. Therefore, GG's results envelop RBS.

A CO pressure time-history was calculated as:

$$\Delta P(t) = \Delta P_{vent}(t) + \Delta P_{sleeve}(t)$$

Where $\Delta P_{vent}(t)$ is the pool pressure time-history as currently defined in the GESSAR II and using the best correlation of Mark III CO frequency and amplitude test data (Reference 9). The term $\Delta P_{sleeve}(t)$ represents the expected pool pressure time-history resulting from CO only in the sleeve. This term was calculated using the same techniques and data correlations as ΔP_{vent} but amplitude and frequency were modified by the scaling assumptions previously described. The sleeve CO pressure time-history was determined to be:

$$\Delta P_{sleeve}(t) = \frac{AMP(t)}{2}$$

$$\{0.8 \sin (2\pi\tau(t) f_s(t)) + 0.3 \sin (4\pi\tau(t) f_s(t)) + 0.15 \sin (6\pi\tau(t) f_s(t)) + 0.2 \sin (8\pi\tau(t) f_s(t)) \}, \text{ psid}$$

where:

$\Delta P_{sleeve}(t)$ = pressure amplitude contribution of the SRVDL sleeve on the drywell wall

AMP (t) = peak-to-peak amplitude variation with time, psid

$$= \sqrt{A_{sleeve}/A_{vent}} \times 5.5 \times PPA_{(G,a,T)}$$

$f_s(t)$ $\frac{D_{h\,vent}}{D_{h\,sleeve}} \times f(G_s, a, T)$

= relative time within each cycle, seconds

= time from initiation of LOCA blowdown, seconds

PPA = CO amplitude correlation on containment wall, psid

f = CO vent frequency correlation

G = sleeve steam mass flux, lb/sq ft/sec

a = vent air content, percent

T = bulk pool temperature, °F

D = hydraulic diameter

A = area

A portion of the resulting pressure time-history on the drywell wall for Grand Gulf is shown in Figure 5-2

(vent CO only) and Figure 5.3 (simultaneous vent and sleeve CO).

Significance of the SRVDL Sleeve CO Load

The pressure time-histories of Figures 5-2 and 5-3 were digitized and ARS plots were prepared. Peak broadening of 15 percent was used, as in the GESSAR II CO load, to account for uncertainty in the predicted frequencies. The ARS resulting from the time-histories given in Figures 5-2 and 5-3 are shown in Figures 5-4 and 5-5. As evident from these plots, the SRVDL sleeve CO has no impact below 30 Hz. Superimposed on Figure 5-5 is the ARS of the chugging load on the drywell wall (Reference 10). In the frequency range of the sleeve CO pressure, signal, the chugging load is bounding by a substantial margin, even though an unrealistically large pressure due to the sleeve CO was utilized and credit was not taken for attenuation of the SRVDL sleeve CO as distance away from the sleeve increases.

Figure 5-4 does not correspond directly to the design basis accident (DBA) ARS presented by Grand Gulf in support of the LOCA Licensing defense. Due to limitations in the existing code, a smaller number of cycles was used in Figure 5-4 to obtain the DBA CO peak response at the low-frequency range than were used in developing the DBA CO ARS. At the high-frequency range, however, the number of cycles used is adequate to reach the peak response and Figures 5-5 and 5-6 adequately represent the maximum amplitudes produced by the high frequency components of the CO load.

To determine the effect of the SRVDL sleeve CO on the containment wall loading, the drywell composite CO loading was attenuated to the containment wall. The resulting ARS is shown in Figure 5-6. As is evident from this curve, the ARS of the pool swell containment wall load definition bounds the combined effect of the main vent CO and the SRVDL sleeve CO Note that the global pool swell load is compared to the local SRVDL CO load, so the additional factor of conservatism previously discussed (on the order of 2) is present.

In summary, a bounding and extremely conservative analysis shows that the CO produced by the SRVDL sleeve adds high frequency components to the basic main vent CO load definition. This additional contribution is bounded by other loads. Also, since the response is increased in only the high frequency range, the structural impact of this loading is very small.

Item 3

Based on analysis for the loading provided in Figure 5-3, the resulting increases in structural forces and moments are not significant and are enveloped by other LOCA cases.

Item 4

A detailed description of the hydrodynamic and thermal loads on the SRVDL piping and the SRVDL sleeve during LOCA blowdown is given below.

SRVDL Piping

1. Inertia loads caused by building excitation. The loading cases include CO, chugging, and pool swell.

2. Drag loads on SRVDL piping, quencher, and quencher supports. The load cases include LOCA vent clearing, LOCA bubble and pool fallback, CO and chugging.

3. Lateral load due to chugging.

4. LOCA caused by the drywell negative pressure transient. The loading conditions include weir impact and weir drag.

5. The thermal loads on the piping are based on drywell and the suppression pool temperature during accident conditions.

SRVDL Sleeve

1. Inertia loads caused by building excitation. The load cases considered are pool swell, CO, and chugging.

2. Drag loads, including LOCA bubble, pool fallback, CO, and chugging.

3. Thermal loads. The thermal loads imposed on the sleeve from steam flow through the annulus have been accounted for in the design.

Items 5 and 6

External drag loads due to the sleeve CO have been generated for the DBA condition. Evaluation of this new sleeve CO drag loads and the thermal loads created by steamflow has been performed. Results showed that

both the SRVDL and the penetration sleeve have sufficient margin to accommodate the new loads. The maximum external pressure loads which the safety relief valve discharge lines (SRVDL) can withstand in the region enclosed by the drywell penetration sleeve are 300 psi (upset) and 450 psi (faulted). These pressures are orders of magnitude higher than maximum calculated drywell pressure.

Item 7

SRVDL sleeve chugging lateral loads on the SRVDL sleeve have been calculated by scaling the Mark III downcomer lateral load data to the outside diameter of the SRVDL sleeve. No credit is taken for the presence of the SRVDL in the bubble, providing a very conservative loading. The scaling base is the Mark II chugging lateral load specified in Reference 15 and given in the following equation.

$$F = 65{,}000 \sin\left(\frac{\pi t}{.003}\right), \quad 0 < t < .003$$

where t = time (sec)
F = lateral load (lbf)

The Mark II load was based on 100 downcomers. Since there are only 16 SRVs in River Bend, only 16 percent of the total number of individual chugs is expected. When the reduced number of chugs is figured into the Mark II load, the peak force reduces from 65,000 lbf to 55,000 lbf.

The revised Mark II load is scaled from Mark II 24-in. vents to the River Bend SRVDL sleeve outside diameter of 14 in. The scaling relation is presented here.

$$\frac{F_1}{F_2} = \left(\frac{D_1}{D_2}\right)^m$$

where F_1, F_2 = lateral load
D_1, D_2 = pipe diameter
m = empirical factor

Reference 14 shows that compilation of the 4T statistical average data results in an exponent of $m = 1.7$. Using this exponent in the above formula with the given SRVDL sleeve outer diameter results in a peak force of 22,000 lbf or 22 kips. The resultant loading equation follows:

$$F = 22{,}000 \sin\left(\frac{\pi t}{.003}\right) \text{ lbf for } 0<t<.003$$

This load is distributed uniformly with a triangular impluse duration of 3 milliseconds on the SRVDL and the SRVDL sleeve. The application lengths are defined by reducing the Mark II values by the ratio of the SRVDL sleeve diameter to the Mark II downcomer diameter. The Mark II values are 1 to 4 ft from the end of the downcomers. The scaled application lengths for RBS are 0.6 to 2.3 ft. These lengths are from the end of the SRVDL sleeve in the wetwell. The piping and SRVDL sleeves for RBS are qualified to the resultant load, impulse duration, and application region given by the above values and methodology to follow.

The Humphrey chugging load (22 kips) was applied to the SRVDL over the applicable regions as follows:

1. 0 to 0.6 ft from sleeve end
2. 0 to 2.3 ft from sleeve end

These chugging results were then combined by the SRSS with the other applicable dynamic loads to obtain the total emergency and faulted loads.

Emergency Load = SRSS (OBEI inertia, SRV inertia, chug/CO inertia, SRV drag, chug/CO drag, and Humphrey chug load)

Faulted Load = SRSS (SSEI inertia, SRV inertia (chug/CO or poolswell) inertia, SRV drag (chug/CO drag and Humphrey chug load))

The resultant stresses, support loads, and equipment loads in the quencher region for these two cases were analyzed in the following manner:

1. Compared with existing stresses and loads for a typical SRVDL/quencher arrangement and found to be less, or

2. Compared with the allowable stresses/equipment loads and found to be less.

The SRV sleeve was qualified by the Class 1 requirements according to the load combination equations of Table 1 of SWEC Specification No. 219.702. First, all the necessary dynamic loads were generated. The dynamic loads from drywell vibration due to OBE, SSE, SRV actuation, CO, chugging, and pool swell were all considered using drywell ARS at el 90 ft 0 in. The drag loads due to SRV bubble, CO, chugging, and pool swell, and GE's lateral loads due to chugging were analyzed using the time-history method. The total loads on the SRVDL sleeve were then

conservatively obtained by taking the absolute sum of the results of the response spectra analysis and the peak of all the time-history analyses for each dynamic load case. From the load combinations examined, it was found that all of the stress as well as the fatigue requirements were satisfied. Therefore, the loads provided impose no problem on the SRVDL sleeve.

The SRVDL sleeve CO lateral loads for the Mark III sleeve geometry are not considered for the RBS design. The Grand Gulf SRVDL sleeve configuration has an unbalanced loaded area at the discharge end of the sleeve, which may introduce a dynamic lateral loading. The River Bend sleeve geometry does not have the unbalanced area. Therefore, there is no CO lateral load. See Figure 5-7 for comparison of sleeve geometries (Reference 13).

Based on this response, this item is considered closed for RBS.

References

1. A. M. Varzaly, et al, Mark III Confimatory Test Program - Test Series 6003, NEDE-24720P, January 1980

2. GESSAR II, Question/Response 3B.11, 22A7000, Rev. 2, 1981

3. River Bend SSER 2, Appendix K, Review of Humphrey Concerns, Pg 6-7

4. MP&L letter No. AEOM 82/574 dated December 3, 1982 from L. F. Dale (MP&L) to H. R. Denton (NRC)

5. "Mark I Containment Program Full-Scale Test Program Final Report", NEDE-24539-P, April 1979

6. "Mark I Containment Program Load Definition Report", NEDO-21888, Revision 2, November 1981

7. W. J. Bilanin, The General Electric Mark III Pressure Suppression Containment System Analytical Mode, General Electric Report No. NEDO-20533, June 1974, and Supplement 1, September 1985

8. General Electric Company, Comparison of Single and Multivent Chugging at Two Scales, NED-24781-1-P, January 1980

9. A. M. Varzaly, et al, Mark III Confirmatory Test Program -1/3 Scale Condensation and Stratification Phenomena - Test Series 5807, General Electric Report No. NEDE-21596-P, March 1977

10. GESSAR II, Figure 3B.18.2, page 3BO.3.2.18, 22A7000, June 1981

11. Dynamic Lateral Loads on a Main Vent Downcomer - Mark II Containment, NEDE-24106-P, General Electric Company, March 1978

12. S. T. Nomanbhoy, Loads on the Vent Struts Due to Condensation of Steam in a Water Pool, NEDE-23627-P, General Electric Company, June 1977

13. General Electric Transmittal, Load Specification for CO Lateral Loads on Mark III SRVDL Sleeve (Response to NRC SER Concerns 2.2 and 2.3, MDE-121-05-85, DRF-T23-500-1, May 1985

14. GE Response to CIRP Question 5.7.1, Chugging Lateral Loads on the SRVDL Sleeve

15. Mark II Containment Program Load Evaluation and Acceptance Criteria, NUREG-0808, August 1981

TABLE 1

SRVDL SLEEVE CO LOADS FOR
RIVER BEND BASED ON MARK I LDR

Frequency Component	Frequency Range (Hz)	Pressure Harmonic Amplitude (PSI) SRVDL Sleeve Annulus	Drywell Wall	Containment Wall
1	24 to 48	3.6	1.33	0.21
2	48 to 96	1.3	0.48	0.08
3	72 to 144	0.3	0.11	0.02

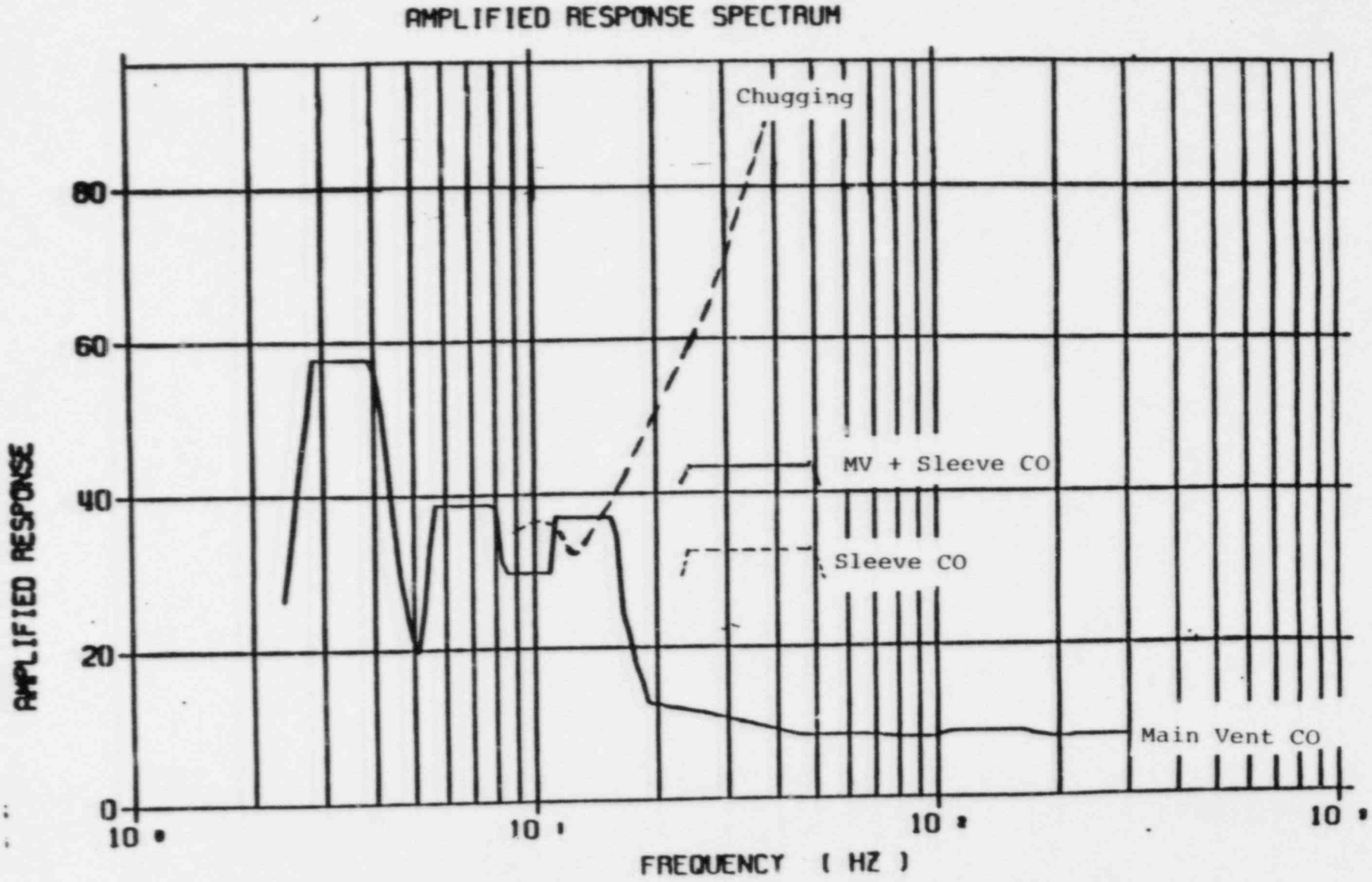

Figure 4 - ARS Comparison on Drywell Wall

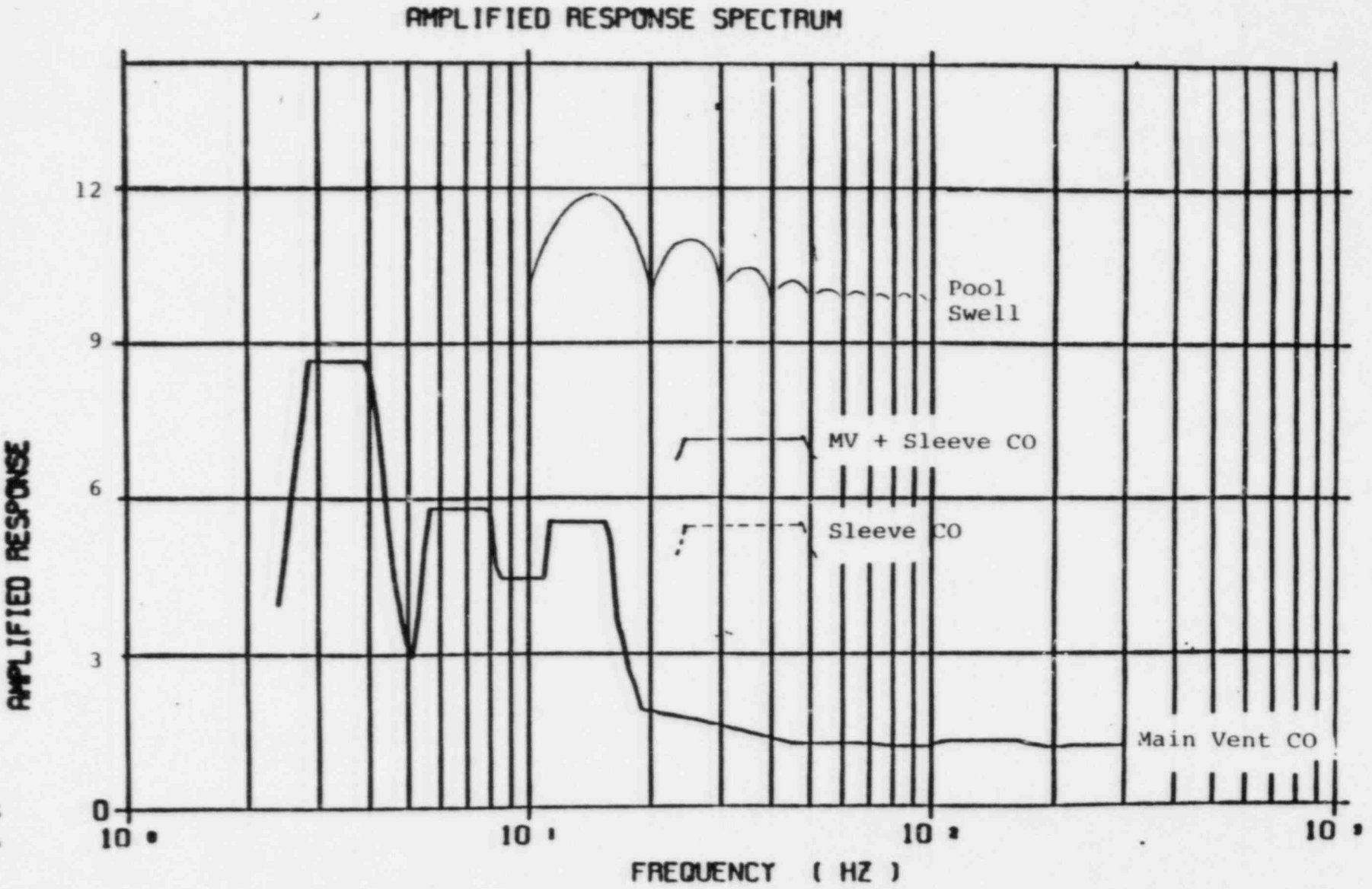

Figure B - ARS Comparison on Containment Wall

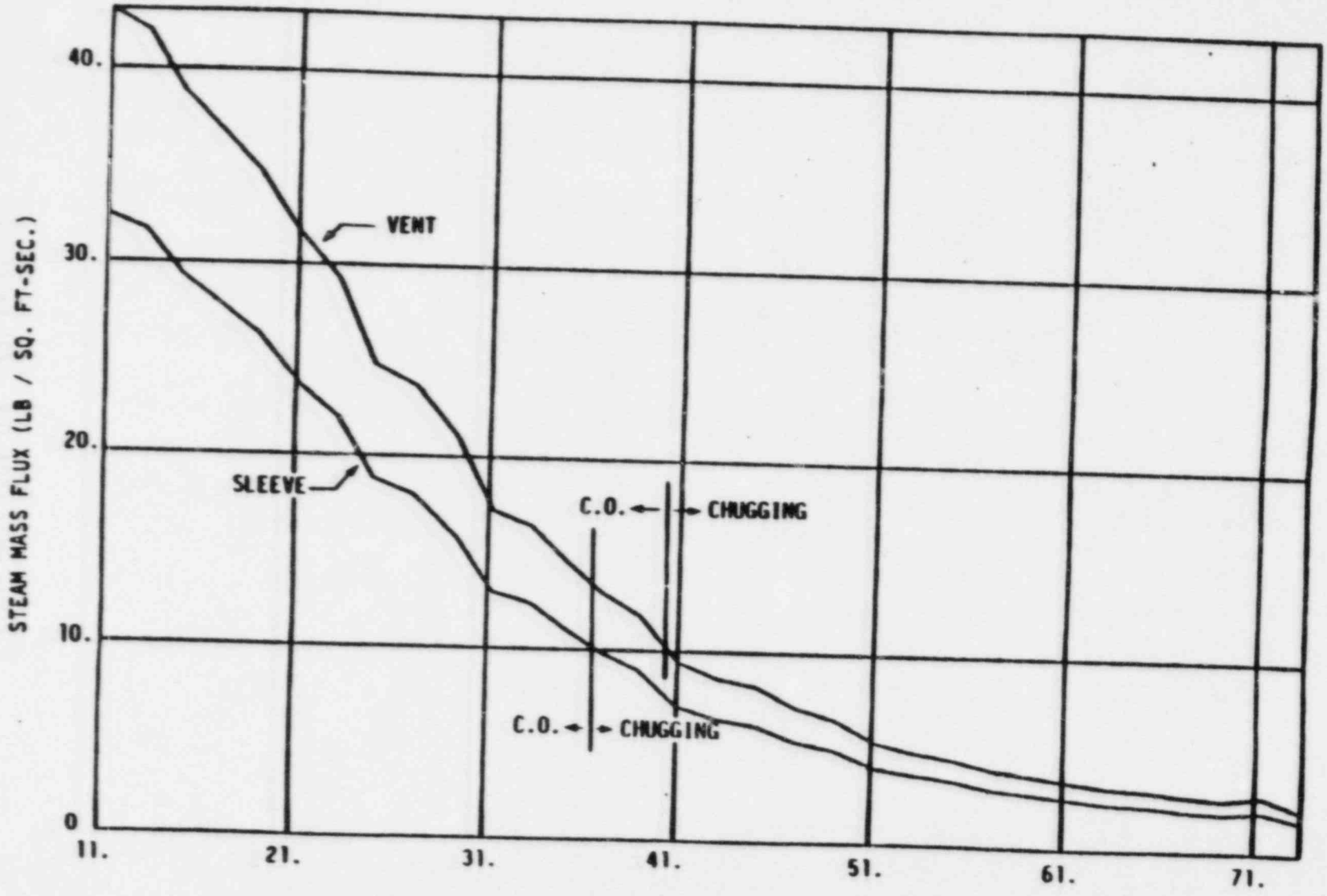

CALCULATED VENT AND SLEEVE STEAM MASS FLUX FOR GRAND GULF 100% BREAK SIZE

FIGURE 5-1

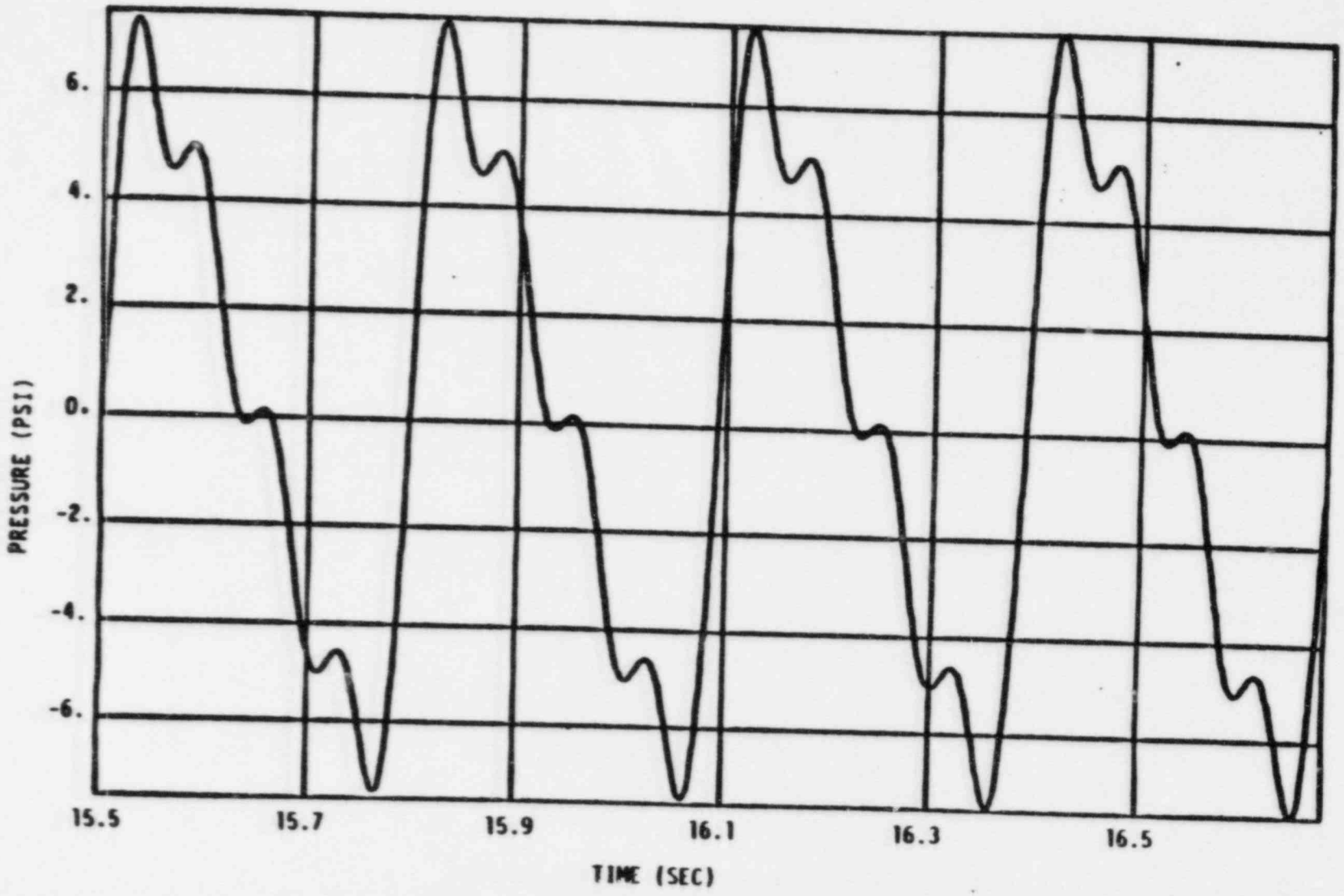

PRESSURE TIME HISTORY WITH C.O. IN THE VENT ONLY

FIGURE 5-2

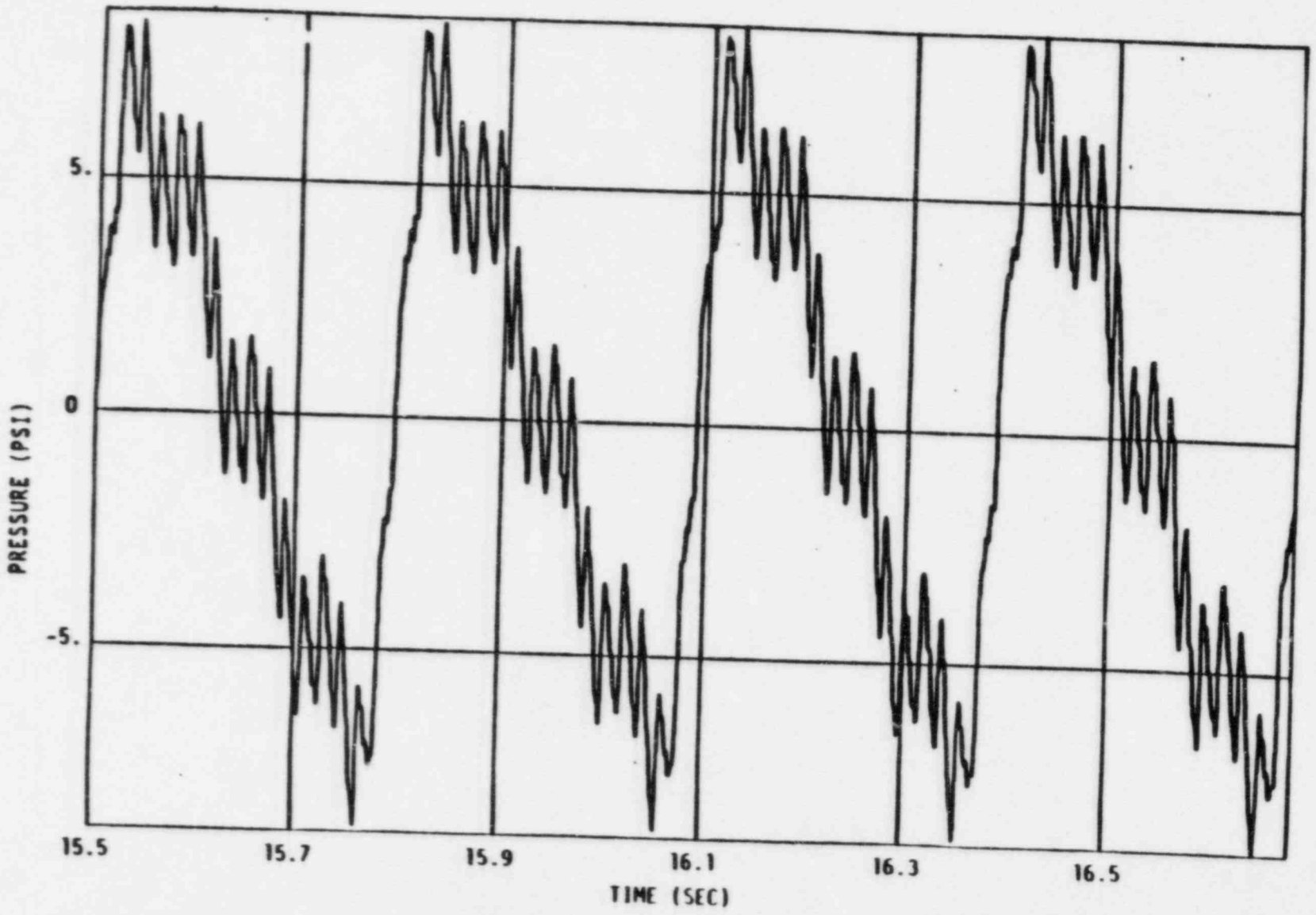

PRESSURE TIME HISTORY ON DRYWELL WALL WITH C.O. IN THE VENT AND THE SRVDL SLEEVE

FIGURE 5-3

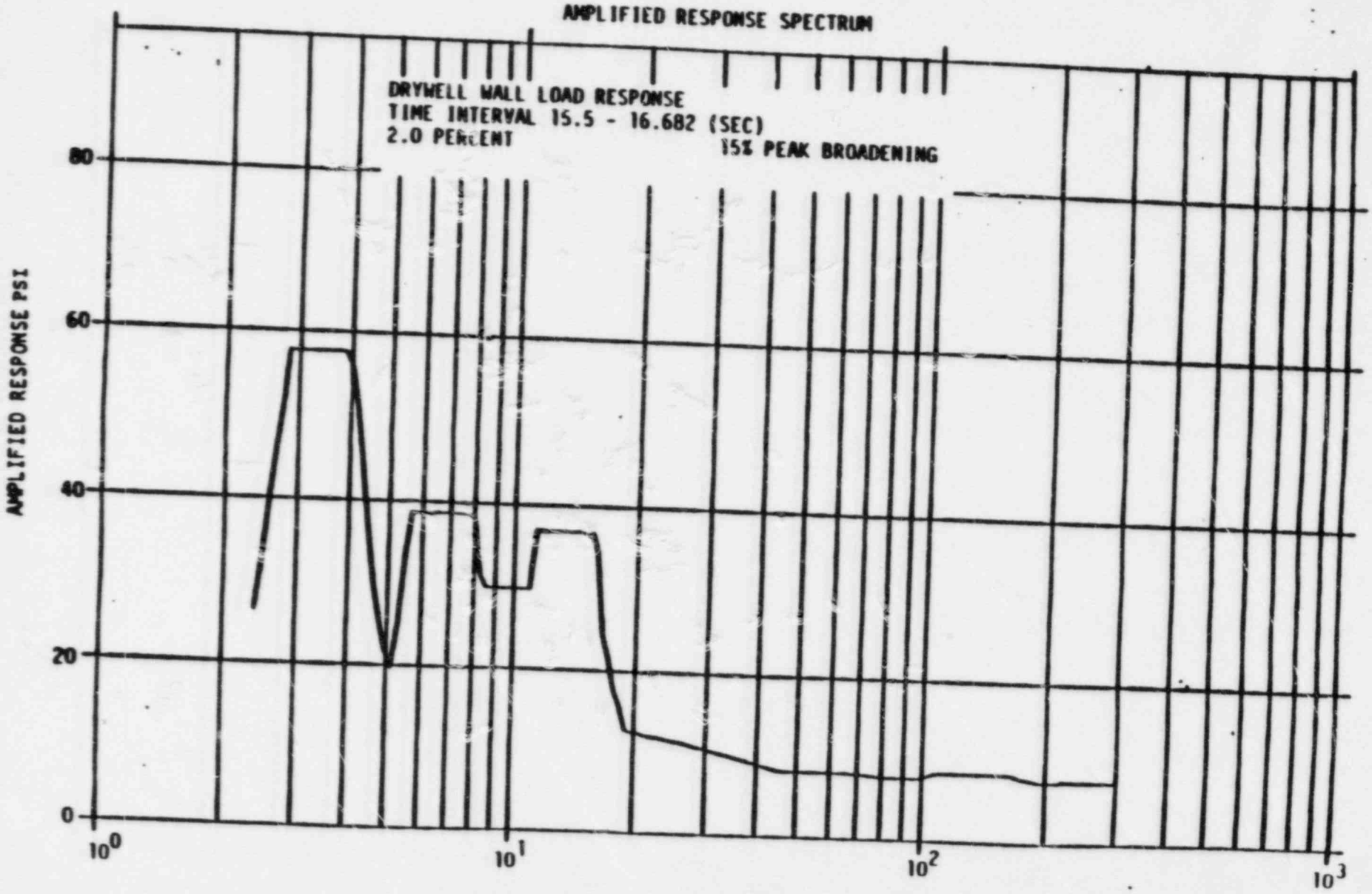

ARS OF PRESSURE TIME HISTORY WITH C.O. IN THE VENT ONLY

FIGURE 5-4

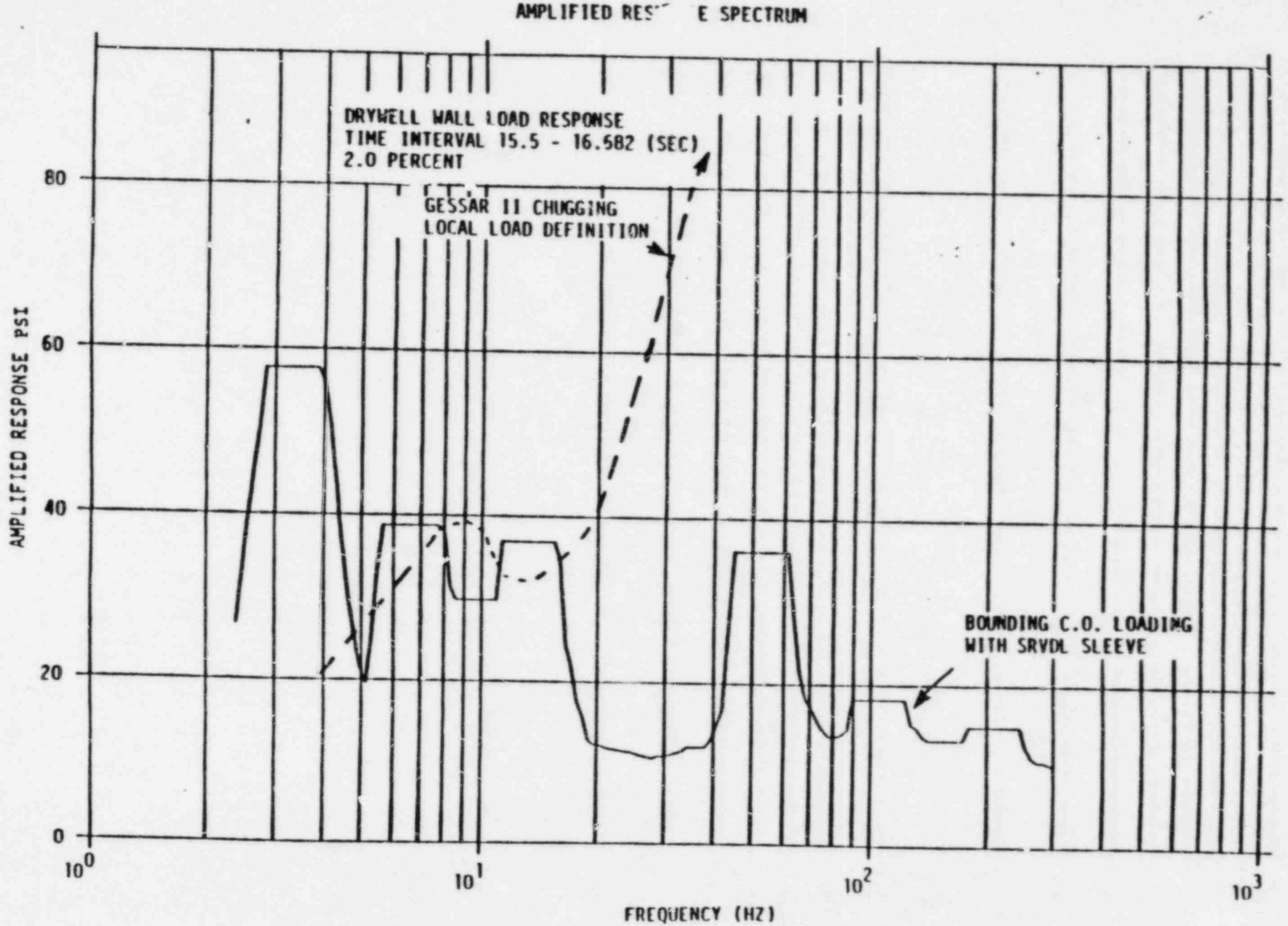

Figure 5-5 COMPARISON OF GESSAR II LOCAL CHUGGING LOAD DEFINITION AND EXPECTED C.O. LOADING WITH SRVDL SLEEVE ON DRYWELL WALL

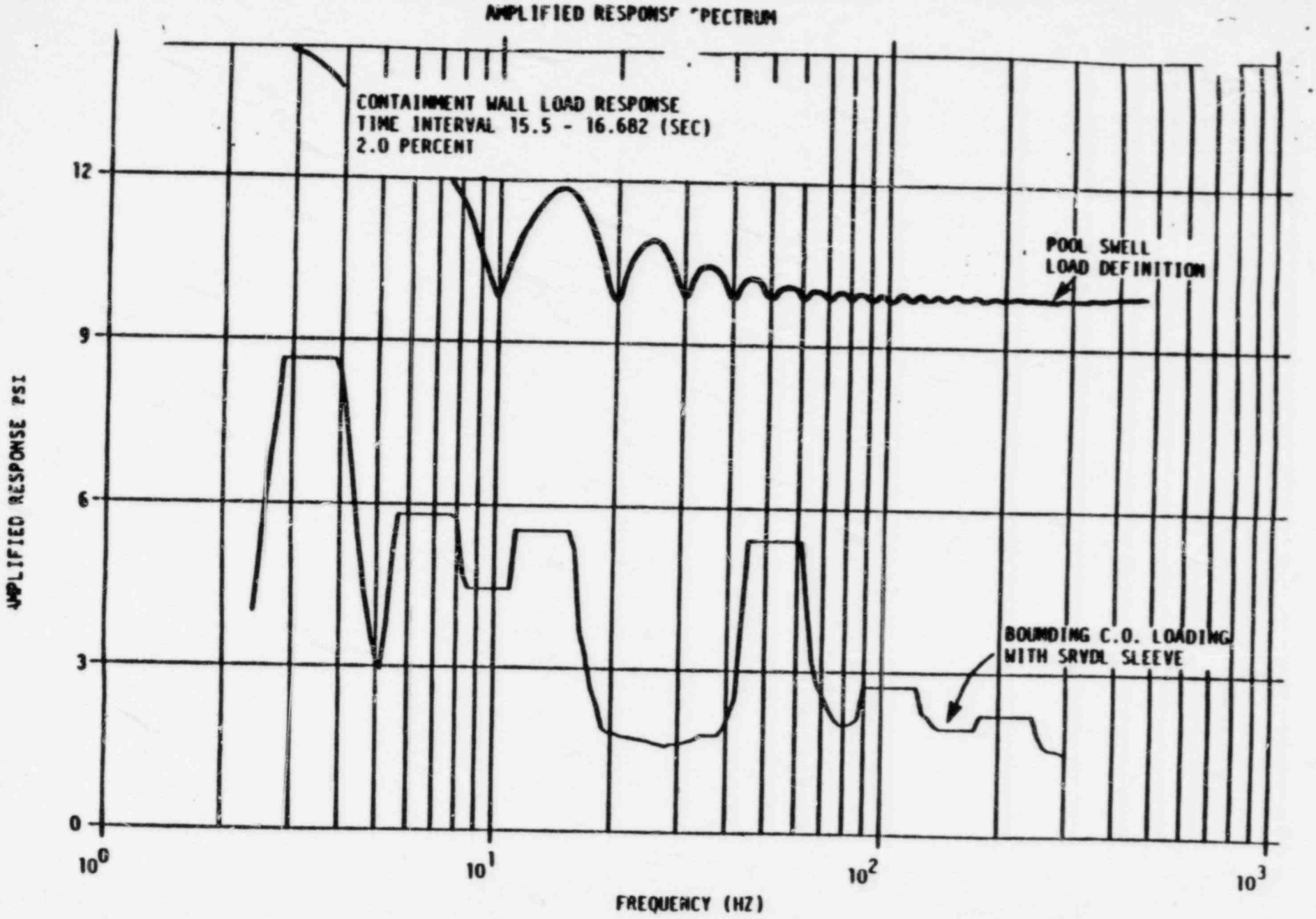

COMPARISON OF POOL SWELL LOAD DEFINITION AND EXPECTED C.O.
LOADING WITH SRVDL SLEEVE ON CONTAINMENT WALL

FIGURE 5-6

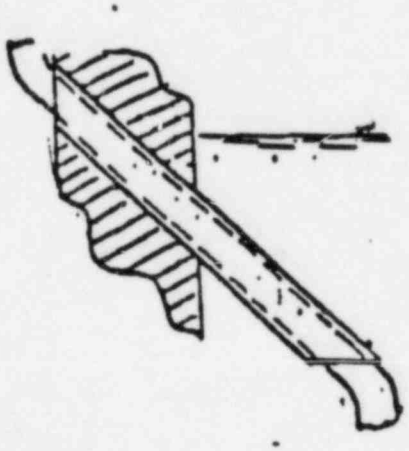

Sketch of the Grand Gulf SRVDL Sleeve

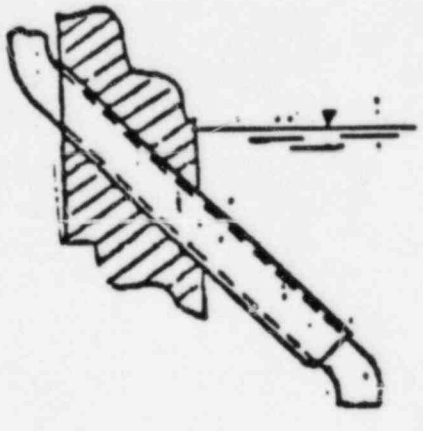

Sketch of the River Bend SRVDL Sleeve

FIGURE 5-7

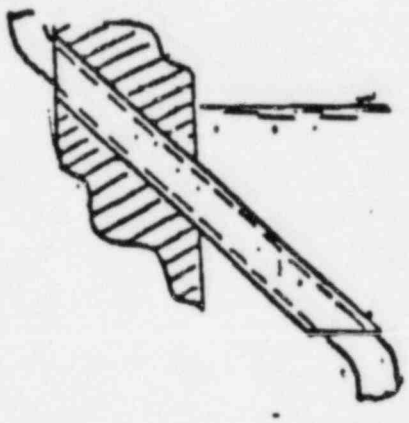

Sketch of the Grand Gulf SRVDL Sleeve

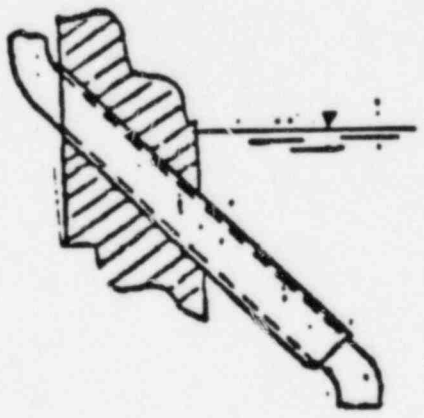

Sketch of the River Bend SRVDL Sleeve

FIGURE 5-7

Action Plan 6 - Plant Specific

I. Issues Addressed

3.1 The design of the STRIDE plant did not consider vent clearing, CO, and chugging loads which might be produced by the actuation of the residual heat removal (RHR) heat exchanger relief valves.

3.3 Discharge from the RHR relief valves may produce bubble discharge or other submerged structure loads on equipment in the suppression pool.

3.7 The concerns related to the RHR heat exchanger relief valve discharge lines should also be addressed for all other relief lines that exhaust into the pool.

II. Program for Resolution*

1. The vent clearing and chugging loads produced by the actuation of the RHR heat exchanger relief valves will be calculated and compared with the main steam SRV bubble loads.

The following information will be submitted for all relief valves that discharge to the suppression pool.

2. The piping drawings and piping and instrumentation diagrams (P&IDs) showing line and vacuum breaker locations will be provided. This information will include the following:

   - The geometry (diameter, routing, height above the suppression pool, etc) of the pipeline from immediately downstream of the relief valve up to the line exit.
   - The maximum and minimum expected submergence of the discharge line exit below the pool surface.
   - Any lines equipped with load-mitigating devices (e.g., spargers or quenchers).

3. The range of flow rates and character of fluid (i.e., air, water, steam) that is discharged through the line and the plant conditions (e.g., pool temperatures) when discharges occur will be defined.

4. The sizing and performance characteristics (including make, model, size, opening characteristics, and flow characteristics) of any vacuum breakers provided for relief valve discharge lines will be noted.

5. The potential for oscillatory operation of the relief valves in any given discharge line will be discussed.

6. The potential for the failure of any relief valve to reseat following initial or subsequent opening will be evaluated.

7. The location of all components and piping in the vicinity of the discharge line exit and the design bases will be provided.

8. The CO load resulting from the RHR heat exchanger relief valve actuation will be calculated and compared with the SRV bubble and LOCA hydrodynamic loads.

III. Status

Items 1 through 8 are considered complete with this submittal.

IV. Final Results*

Analysis was performed for the RHR heat exchanger relief valve actuation line. It was found that the vent clearing load produced by the actuation of the RHR heat exchanger relief valves has been calculated without considering the steam venting effect of the noncondensible vent. Vent clearing and steam condensation loads produced by RHR RV actuation were analyzed as follows.

RHR air bubble pressure-time history is developed based on the bubble dynamics of oscillating air bubbles in the finite pool as described in GESSAR for vent clearing. For this case, initial pressure and velocity are equal to the exit pressure and velocity of the air bubble. The initial pressure and velocity of the air bubble are obtained from the steam hammer computer program analysis (FSAR Appendix 3A). The maximum peak pressure of the RHR air bubble is 12.78 psi. This value is bounded by the SRV air bubble pressure of 16.56 psi (reference FSAR Table A.6A.5-1).

In order to determine source pressure for RHR-induced condensation oscillation (RHR CO) and chugging, a Mark III model is used which represents the suppression pool as an acoustic medium. The low steam mass flux value was used to generate the dynamic pressure on the containment walls of a cylindrical or annulus pool due to a point disturbance. By solving a three-dimensional acoustic wave model, with pool

walls assumed as rigid boundaries and the pool surface as a constant pressure boundary, pressure fields produced by distributed point sources can be found in the suppression pool. The peak dynamic pressure generated for CO is 8.17 psi. This value is considerably smaller than the SRV air bubble peak dynamic pressure. The maximum peak pressure oberved for chugging at the RHR tee elevation is 1.01 psi, which is approximately 16 times lower than the maximum pressure experienced by the SRV bubble.

In conclusion, for RHR air bubble, RHR CO, and chugging events, the peak dynamic pressures generated are bounded by the SRV air bubble peak dynamic pressure of 16.56 psid. Furthermore, the RHR bubble load frequency is about 7.5 Hz, which is enveloped by the SRV bubble load design frequency of 5 to 12 Hz. Thus, the vent clearing load due to RHR heat exchanger relief valve discharge is not a concern for the RBS containment.

The majority of the information described in Items 2 through 7 is included in the attached tables and the attached FSAR Figures 5.4-12, 6.3-1, and 6.3-4; piping Drawing Nos. 12210-EP-71A, 71F, 83A, and 13A; and valve Drawing No. 12210-0228.213-058-001G. The minimum and maximum suppression pool levels are 89 ft 6 in. and 90 ft 0 in., respectively. None of the relief valve discharge lines have a load-mitigating device, because they discharge only water into the suppression pool, except for RHR steam relief valves 1E12*RVF055A and B and 1RHS*RV3A and B, which are addressed in this Action Plan.

When RHR pressure control valves 1E12*PVF051A and B begin to cycle in an undefined manner, the RHR heat exchanger relief valves experience cyclic behavior. However, the vent valves which pressurize this relief valve discharge line in the steam-condensing mode depress the water leg out of the piping. Additionally, since the most rapid travel time for the RHR pressure control valve is 10.5 sec as a result of the valve design, any postulated oscillation would be quite slow.

There is also a possibility that the RHR heat exchanger relief valve may fail to open during RHR system operation or that the relief valve may fail to reseat following normal actuation. The water hammer analyses performed for Action Plan 8, Program for Resolution, Item 2 will bound all conditions associated with the postulated failure of any relief valve discharging to the suppression pool.

Drawing No. EP-71A shows components in the vicinity of the RHR heat exchanger relief valve discharges. The loads produced by discharge from these relief valves will bound all postulated loads which could be produced by other relief valves discharging to the suppression pool, including the LPCS relief valves which discharge through these lines. The GE design

criteria for the HPCS and LPCS strainers, given in the HPCS and LPCS design specifications, require them to be located at least 8 ft from the discharge of the main steam safety relief valve ram's head. While River Bend does not use a ram's head on the main steam safety relief valves, this criteria is applicable to the RHR relief valves since the ram's head configuration, an open-ended pipe, is similar to the RHR relief valve discharge lines. Since the flow from the RHR heat exchanger relief valves is much less than the main steam safety relief valves, the present design is acceptable. Drawing No. EP-83A shows that the flow from valves of components in the vicinity of the HPCS relief valves is low, and submerged structure loads are negligible.

For RBS Unit 1, RHRDL vent clearing water jet loads, air bubble, and CO loads have been derived and evaluated in the following manner:

1. During the water jet event, the ejection of water induces an unsteady flow field causing hydrodynamic loads on piping and supports. The Mark II methodology is applied to calculate the jet flow field using the following potential function:

$$\phi = \frac{3}{8\pi} Uj\ Vw \frac{Cos\theta}{r^2}$$

Where ϕ represents velocity potential function; r and θ are the spherical coordinates from the jet front center, with 0 measured from the jet direction; Uj is the jet front velocity; and Vw is the initial volume of the water in the RHRDL. Initial volume is based on results obtained from the reflood analysis. Once the flow field is known, the velocity and acceleration drags are calculated on the affected structures using Morrison's equation. The total drag load is given as the algebraic sum of the velocity and acceleration drag.

2. Following the water clearing phase, pressurized air in the form of an air bubble is purged into the suppression pool. This event creates unsteady fluid motion with the pool area, causing hydrodynamic loads on the submerged structures. Loads are computed by applying the theory of potential flow to solve the flow field produced by the disturbance of point source. The method of images (MOI) is incorporated into the flow field solution to account for the defined pool boundaries. Since MOI is applicable for the flat boundaries, the annular pool is unfolded into a rectangular box. The source strength of the RHR air bubble is developed based on the air bubble

dynamics using the method outlined in FSAR Section L.6A.2.3 for LOCA air bubbles. This calculated source strength is used to calculate velocity and acceleration drag loads by using Morrison's equation. The total drag is given as the albegraic sum of the velocity and acceleration drags, and the resultant drag is the SRSS of the components.

3. Similarly, hydrodynamic loads on submerged structures due to RHR CO are calculated using the procedure described for RHR air bubble loads, although the source strength is based on a value specified by GE (Reference 1).

   It is found that the hydrodynamic loads on submerged structures due to water clearing, RHR air bubble, and CO events are bounded by SRV bubble loads, although exceptions did occur in each event. The structures that were not bounded by SRV air bubble are analyzed to evaluate the response of the structures.

RBS has participated in a generic Mark III containment evaluation program for the RHR CO. The Grand Gulf Nuclear Station (GGNS) containment was selected as a representative case by the Containment Issue Owner's Group (CIOG). Comparison was made between the RHR CO and the SRV load definition. It is found that the maximum positive pressure due to a single SRV actuation exceeds that due to RHR CO, except in a small region on the containment in the neighborhood of the RHR discharge point and that the actuation of all SRVs produces a peak positive pressure that exceeds the maximum positive pressure generated by RHR CO. Thus, it is concluded that the RHR CO load is bounded by the design basis SRV load specification based on the similarity between the RBS and GGNS containments. The results presented for the RBS CO load calculations also show that the SRV loads are bounding. Therefore, RHR CO load is not a concern to the RBS containment.

Lateral loads are produced by asymetrical bubble collapse. The load magnitude is a function of bubble size, pool temperature, and steam mass flux per unit area. The lateral load specification for RHR discharge piping is defined by using the extensive Mark II straight vent data base and geometrically scaling it to the RHR discharge line outer diameter. The base load of 65 kips is applied with a triangular impulse duration of 3 milliseconds, which was the worst observed in domestic and foreign test data (Reference 2). It envelops all possible combinations of pool temperature and steam mass flux per unit area.

The RBS RHR discharge tee is horizontally symmetric. The tee would actually carry the steam bubble farther away from the pipe. Therefore, it is conceivable that the "impact load" induced on the pipe could be less severe than a straight pipe geometry. Therefore, using the Mark II main vent lateral load data base is conservative. This is further evidenced by the fact that no reportable lateral load incidents were noted in a Mark I plant with a ramshead-equipped SRVDL, including leaky valves or SRV reseat where steam mass flux is low.

Lateral loads were determined by scaling the Mark II downcomer lateral load data to the outside diameter of the RHR discharge line. The scaling base is the Mark II chugging lateral load specified in the following equation:

$$F = 65{,}000 \sin\left(\frac{\pi t}{.003}\right), \quad 0 < t < .003$$

The Mark II load is scaled from Mark II 24-in. vents to the RBS RHRDL outside diameter of 12.75 in. The scaling relationship is presented here.

$$\frac{F_1}{F_2} = \left(\frac{D_1}{D_2}\right)^m$$

where: F_1, F_2 = lateral loads
D_1, D_2 = pipe diameter
m = empirical factor

The application lengths were determined by reducing the Mark II values by the ratio of the RHRRVDL diameter to the Mark II downcomer diameter. This scaling approach results in peak pressures on the RHRRVDL that are comparable to those obtained from the reference Mark II lateral load and application length. The maximum resultant load magnitude for RBS is 22.2 kips over an application region of 0.53 to 2.13 ft.

The lateral loads are distributed uniformly over the RHR discharge line along the application length specified with a triangular impulse duration of 3 milliseconds. These lengths are considered from the centerline of the RHRRVDL pipe tee to the length specified for application. The RHR discharge lines at RBS are qualified to this load and application region.

Resultant stresses from Humphrey chugging loads for the RHRRVDL are combined by the SRSS method with OBEI inertia only for the emergency condition and SSEI inertia only for

the faulted condition. These stresses are then compared with the allowable stresses for each condition and found to be acceptable.

Pipe supports and penetrtations were qualified by their respective groups.

Table 6.1 presents the relief valves included on the RHR discharge lines. Except for RHR steam relief valves 1E12*RVF055A and B and 1RHS*RB3A and B, all other RHR relief valves discharge only water into the suppression pool.

Significant loads on the suppression pool are not expected due to RCIC turbine exhaust pipe discharge. Operating experience and test data indicate stable system performance has been achieved by the implementation of vacuum breakers and a condensing sparger on the RCIC turbine exhaust lines. Since the addition of these devices, there have been no reported instances of excessive exhaust line loads due to system operation (Reference 3). Therefore, since the RBS plant design includes the vacuum breaker and condensing sparger on the RCIC turbine exhaust line, it is expected that significant loads on the suppression pool will not exist.

Based on the above discussion, this issue is considered closed for RBS.

References

1. Enercon Services, Inc., Letter No. RWE-OG-102, from R. W. Evans to L. England, Bechtel RHR Condensation Oscillation Source Report, dated February 20, 1985

2. J. R. Lehner and A. A. Sonin, "Determining a Lateral Load Specification During Chugging in a Mark II Containment," Structural Mechanics in Reactor Technology, Vol J, August 22-26, 1983, pp 75-80

3. Enercon Services, Inc., Letter No. JRC-OG-142, from J. R. Corn to L. A. England, History of Development of the RCIC Exhaust Sparger, dated April 10, 1985

*This revision replaces the GSU submittal dated January 23, 1985

TABLE 6-1

ECCS Relief Valve Discharge into Suppression Pool - Design Conditions

Valve I.D. No.	System	Size (in.)	Relief Flow (lbm/hr)	Set Press. (psig)	Discharge Line Number	Function (Component Protected)	Relief Mode	R/V Inlet Temp. (°F)	Discharged Fluid	Minimum (1) Submergence (ft)
E12-F055A	RHR	4x6	1.3x10⁶	500	1RHS-012-148-2	RHR HX A	Steam Condensing	480	Steam	5 1/2
E12-F055B	RHR	4x6	1.3x10⁶	500	1RHS-012-145-2	RHR HX B	Steam Condensing	480	Steam	5 1/2
1RHS*RV3A	RHR	4x6	1.3x10⁶	485	1RHS-012-148-2	RHR HX A	Steam Condensing	480	Steam	5 1/2
1RHS*RV3B	RHR	4x6	1.3x10⁶	485	1RHS-012-145-2	RHR HX B	Steam Condensing	480	Steam	5 1/2
E12-F025A	RHR	1 1/2x2	6.97x10⁴	500	1RHS-012-148-2	RHR Pump A Disch.	Surveillance Test	358	WATER	5 1/2
E12-F025B	RHR	1 1/2x2	6.97x10⁴	500	1RHS-012-145-2	RHR Pump B Disch.	Surveillance Test	358	WATER	5 1/2
E12-F025C	RHR	1 1/2x2	6.97x10⁴	500	1RHS-012-145-2	RHR Pump C Disch.	Surveillance Test	358	WATER	5 1/2
E12-F005	RHR	3/4x1	6.75x10³	200	1RHS-012-148-2	RHR Shutdown Suc.	Shutdown Cooling	358	WATER	5 1/2
E12-F036	RHR	6x8	7.38x10⁶	75	1RHS-012-148-2	RHR Shutdown Disch.	Steam Condensing	140	Water	5 1/2
E12-F017A	RHR	3/4x1	6.75x10⁴	200	1RHS-012-148-2	RHR Pump A Suc.	System Standby	358	WATER	5 1/2
E12-F017B	RHR	3/4x1	6.75x10⁴	200	1RHS-012-145-2	RHR Pump B Suc.	System Standby	358	WATER	5 1/2
E12-F101	RHR	3/4x1	7.5x10⁴	150	1RHS-012-145-2	RHR Pump C Suc.	System Standby	212	WATER	5 1/2

TABLE 6-1 (CONT)

Valve I.D. No.	System	Size (In.)	Relief Flow (lb/hr)	Set Press. (psig)	Discharge Line Number	Function (Component protected)	Relief Mode	R/V Inlet Temp. (°F)	Discharged Fluid	Minimum (1) Submergence (ft)
E12-F030	RHR	3/4x1	6.75×10^4	200	1PHS-012-145-2	RHR Plumbing RHR	Thermal R/V	212	WATER	5 1/2
E21-F010	LPCS	1 1/2x2	5.01×10^4	570	1PHS-012-148-2	LPCS Pump Disch.	Accident Conditioning	185	Water	5 1/2
E21-F031	LPCS	1 1/2x2	5.01×10^3	100	1PHS-012-148-2	LPCS Pump Suc.	System Isolation	185	Water	5 1/2
E22-F014	HPCS	3/4x1	9.02×10^3	100	1CHS-010-18-2	HPCS Pump Suc.	System Standby	185	Water	12 1/2
E22-F035	HPCS	3/4x1	Thermal R/V	1560	1CHS-010-18-2	HPCS Pump Disch.	Accident Conditions	185	Water	12 1/2
E22-F039	HPCS	3/4x1	Thermal R/V	1560	1CHS-010-18-2	Test Line R/V	Thermal R/V	185	Water	12 1/2
(2)RCIC Turbine	RCIC	-	302×10^4	-	(3)1ICS-012-52-2	Turbine Exhaust	-	250	Steam	8 1/2

(1)Maximum submergence is 5 1/2 ft more than minimum submergence.
(2)Not an ECCS relief valve
(3)This line is equipped with a sparger (1840 1/2 in. diameter holes)

TABLE 6-2

Vacuum Breaker Data

Velan 3/4-In. Spring-Loaded Piston Check Valve
(Drawing No. 0228.213-058-001G)

Disc area - 0.3068 sq in.
Flow area - 0.3068 sq in.
Full open flow coefficient - Cv = 3.2
Maximum disc travel - Approximately 1/4 in.

Valve Mark Nos. E12*VF103A, B, E12*VF104A, B
Function - RHR Relief Valve Discharge Line Vacuum Breakers

TABLE 6-3

Components and Piping in the Vicinity of the Discharge Line Exit

	Centerline Coordinates			
	X	Y	Z	Minimum Distance
1RHS-012-148-2				
Discharge point	40'-7 7/8"	82'-2"	40'-7 7/8"	-
1CSL*STR1(J-)	44'-11 9/16"	76'-6 1/2"	36'-4 15/16"	9'-7 1/4"
1RHS* PSR3013	40'-3 3/4"	73'-4 3/4"	35'-10 1/3"	9'-9 3/8"
1RHS-020-56-2	38'-10 9/16"	73'-4 3/4"	38'-10 9/16"	10'-1 1/16"
1T23*G024S	30'-10 5/8"	75'-7 2/3"	32'-0 7/16"	11'-7 1/8"
1RHS-012-145-2				
Discharge point	40'-7 7/8"	82'-2"	-40'-7 7/8"	-
1RHS-020-1-2	40'-7 7/8"	73'-4 3/4"	-40'-7 7/8"	9'-9 1/4"
1T23*G024L	35'-2 11/16"	75'-7 2/3"	-27'-2 3/8"	12'-8"
1CSH*STR1(J-)	39'-5 1/2"	78'-7"	-42'-3 3/4"	7'-8 3/4"
1CSH-010-18-2				
Discharge point	49'-1"	77'-0"	-30'-3 1/4"	-
1ICS-012-52-2	47'-3 1/3"	71'-3 1/2" on up to 82'-5 1/2"	-29'-6 1/2"	1'-11 1/3"
1RHS-020-1-2	47'-8"	73'-4 3/4"	-29'-4 3/4"	3'-2 3/4"

TABLE 6-3

	Centerline Coordinates			
	X	Y	Z	Minimum Distance
1RHS*PSR3036	48'- 11 2/3"	73'- 4 3/4"	-26'- 5 1/2"	3'- 5 1/2"
1ICS*PSR3001	47'- 3 1/3"	75'- 3 3/4"	-29'- 6 1/2"	2'- 7 1/3"

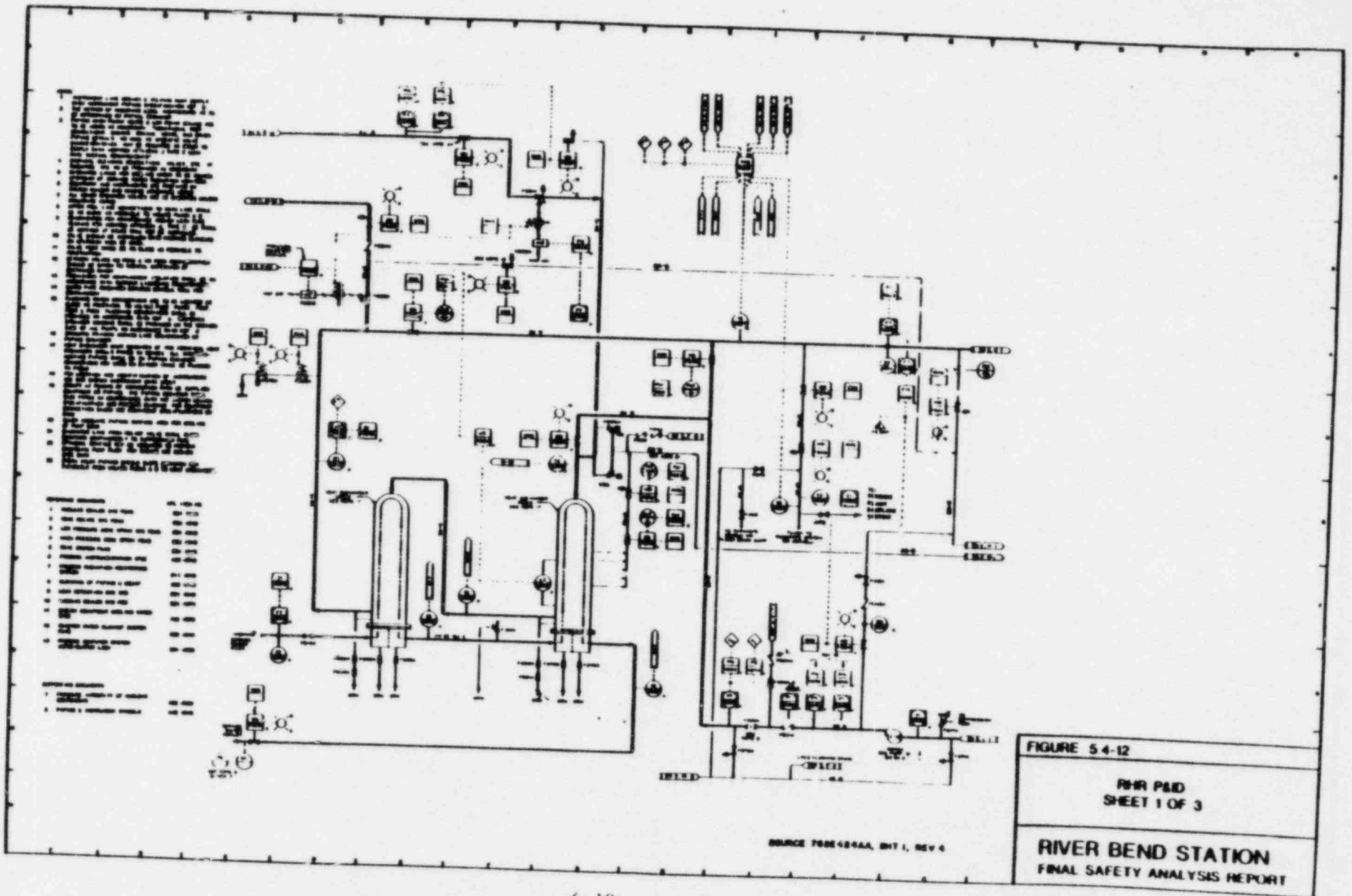

FIGURE 5.4-12

RHR P&ID
SHEET 1 OF 3

RIVER BEND STATION
FINAL SAFETY ANALYSIS REPORT

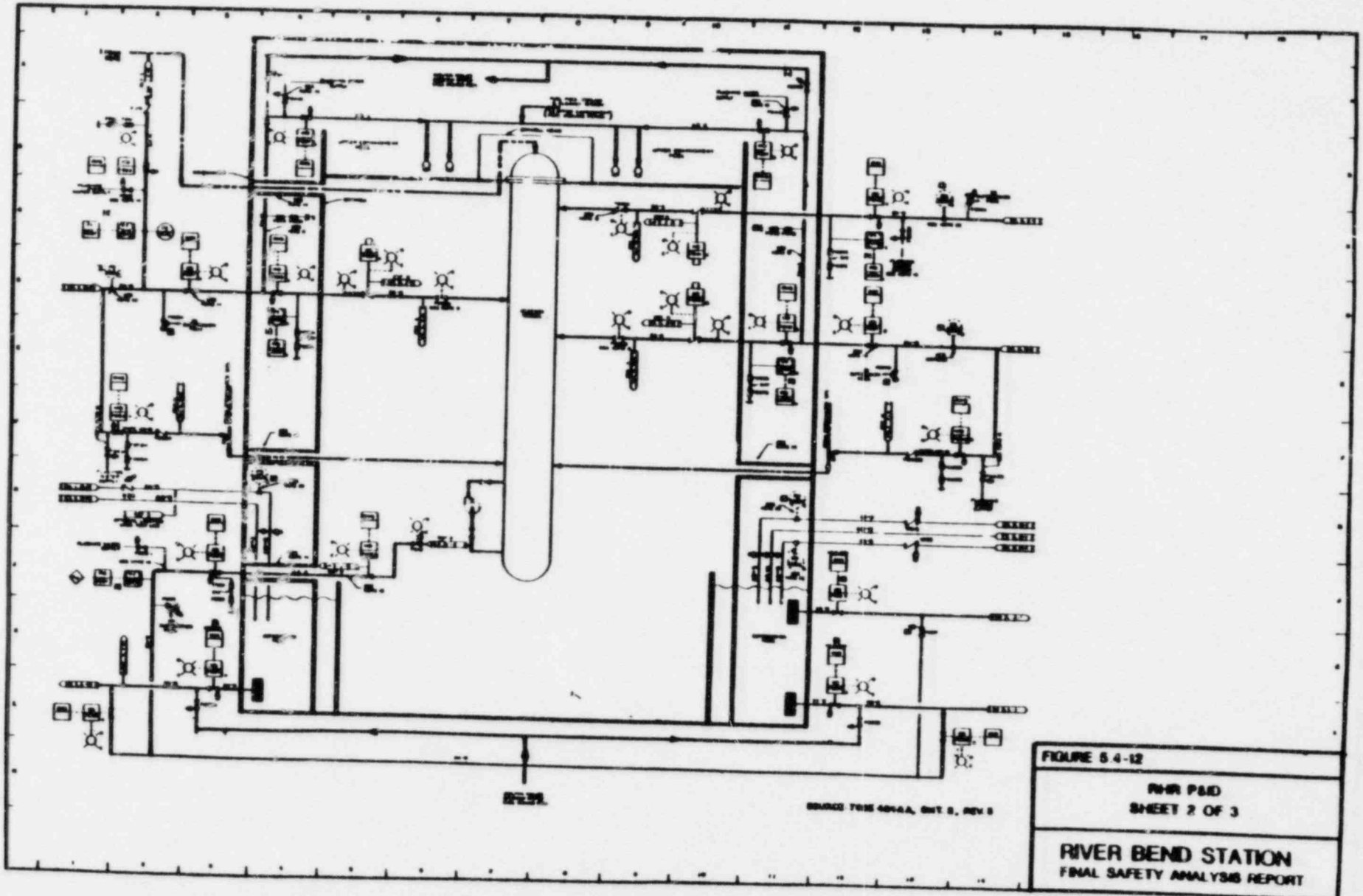

FIGURE 5.4-12

RHR P&ID
SHEET 2 OF 3

RIVER BEND STATION
FINAL SAFETY ANALYSIS REPORT

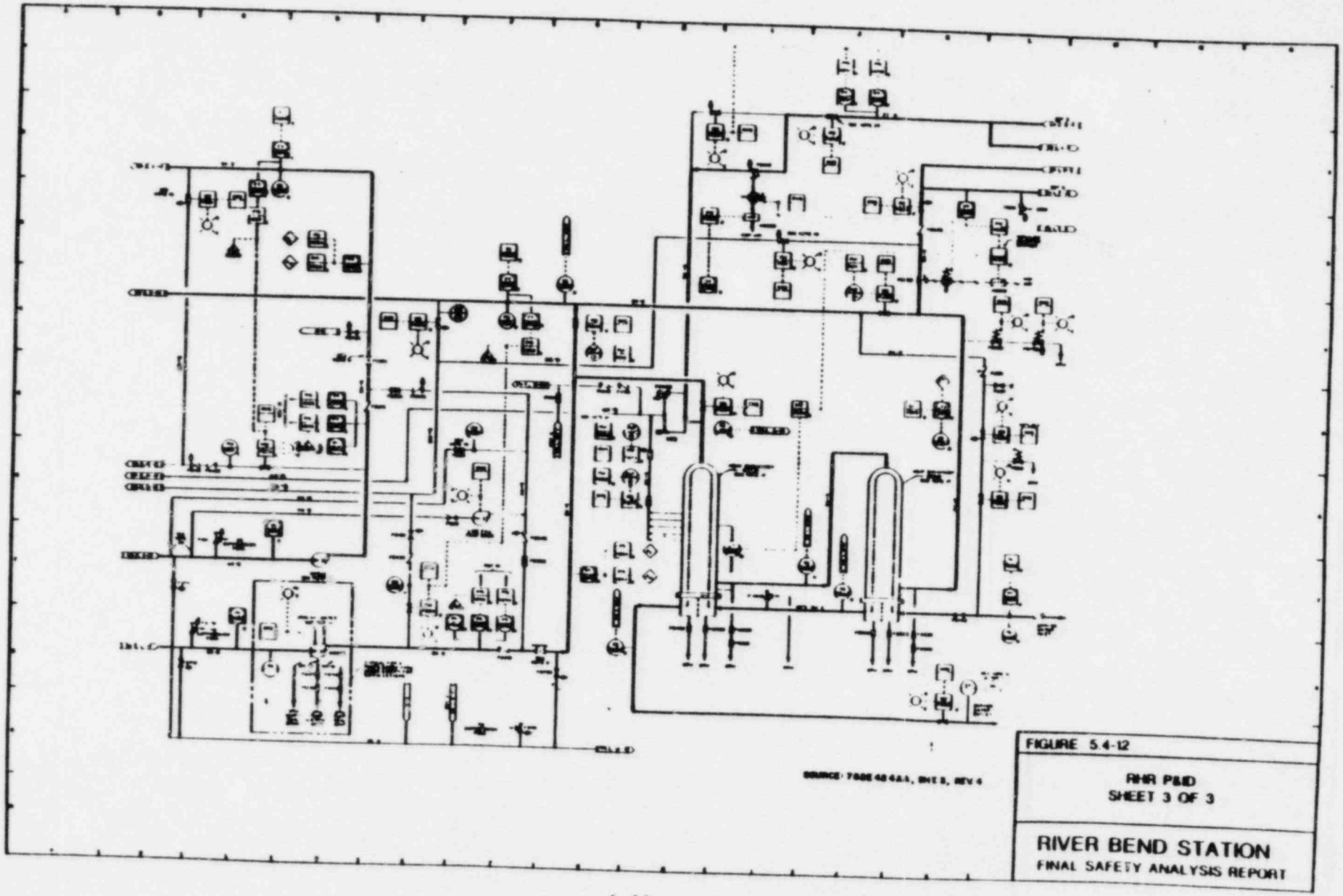

FIGURE 5.4-12

RHR P&ID
SHEET 3 OF 3

RIVER BEND STATION
FINAL SAFETY ANALYSIS REPORT

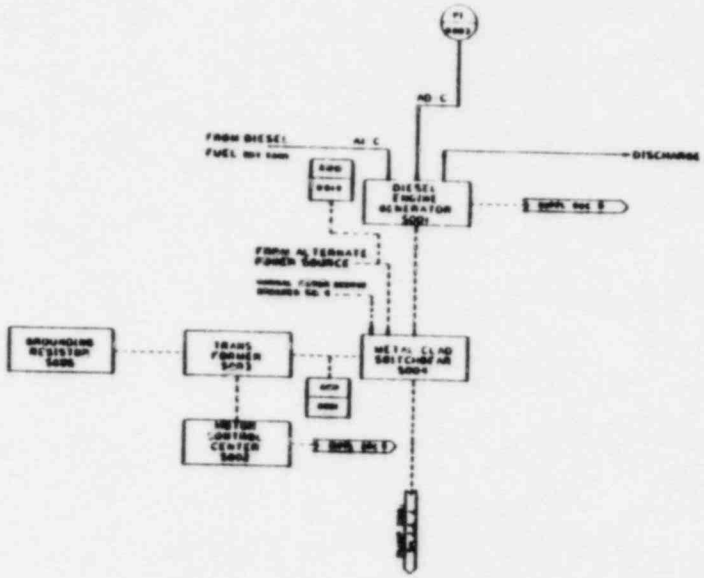

SOURCE 106050ESAA, SH. 1 OF 2, REV 0

FIGURE 6.3-1

HIGH PRESSURE CORE SPRAY SYSTEM P&ID SHEET 1 OF 2

RIVER BEND STATION
FINAL SAFETY ANALYSIS REPORT

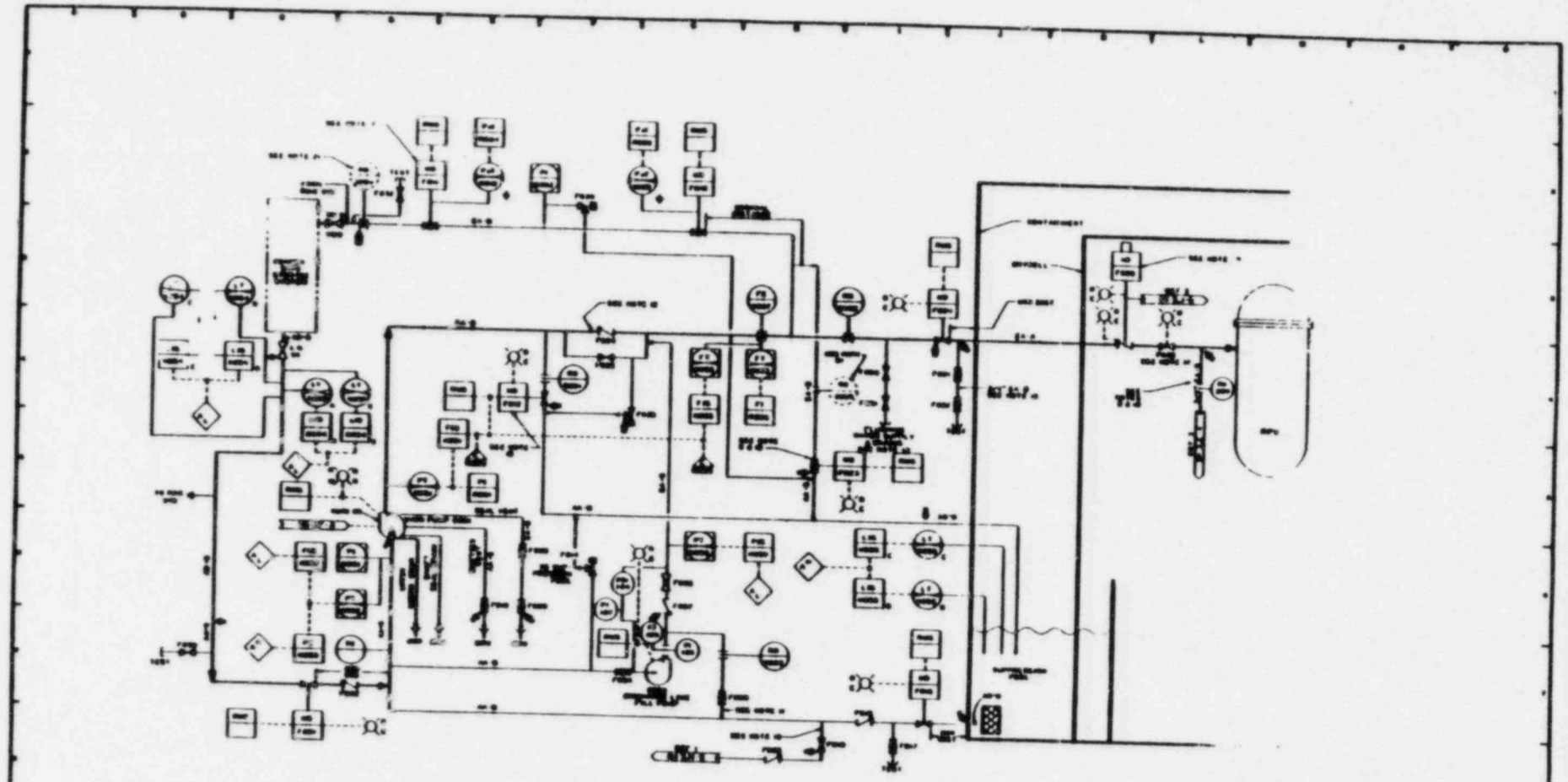

SOURCE 105050E5AA, SH. 2 OF 2, REV 0

FIGURE 6.3-1

HIGH PRESSURE CORE SPRAY SYSTEM P&ID SHEET 2 OF 2

RIVER BEND STATION
FINAL SAFETY ANALYSIS REPORT

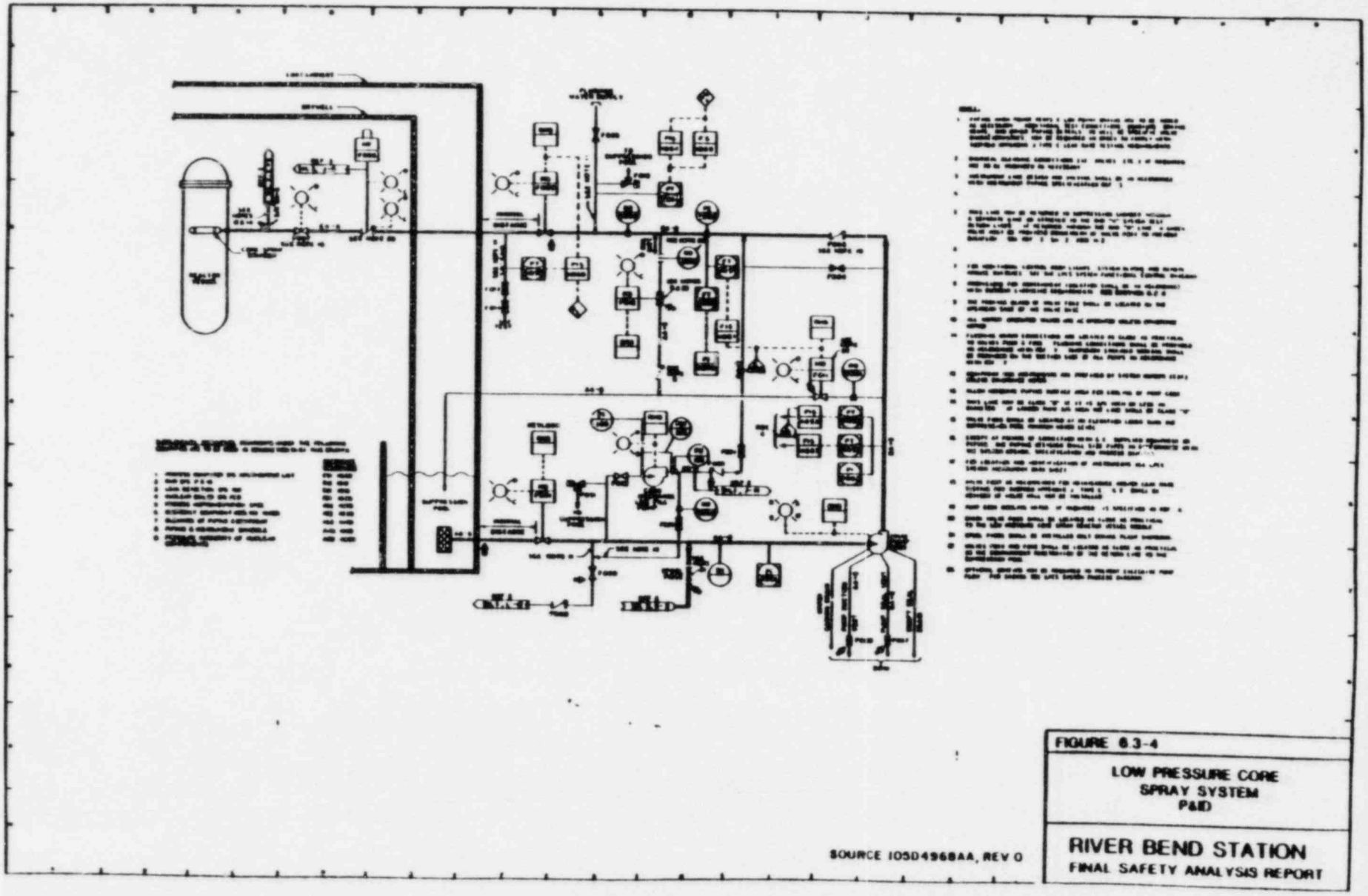

SOURCE 105D4968AA, REV 0

FIGURE 6.3-4

LOW PRESSURE CORE SPRAY SYSTEM P&ID

RIVER BEND STATION
FINAL SAFETY ANALYSIS REPORT

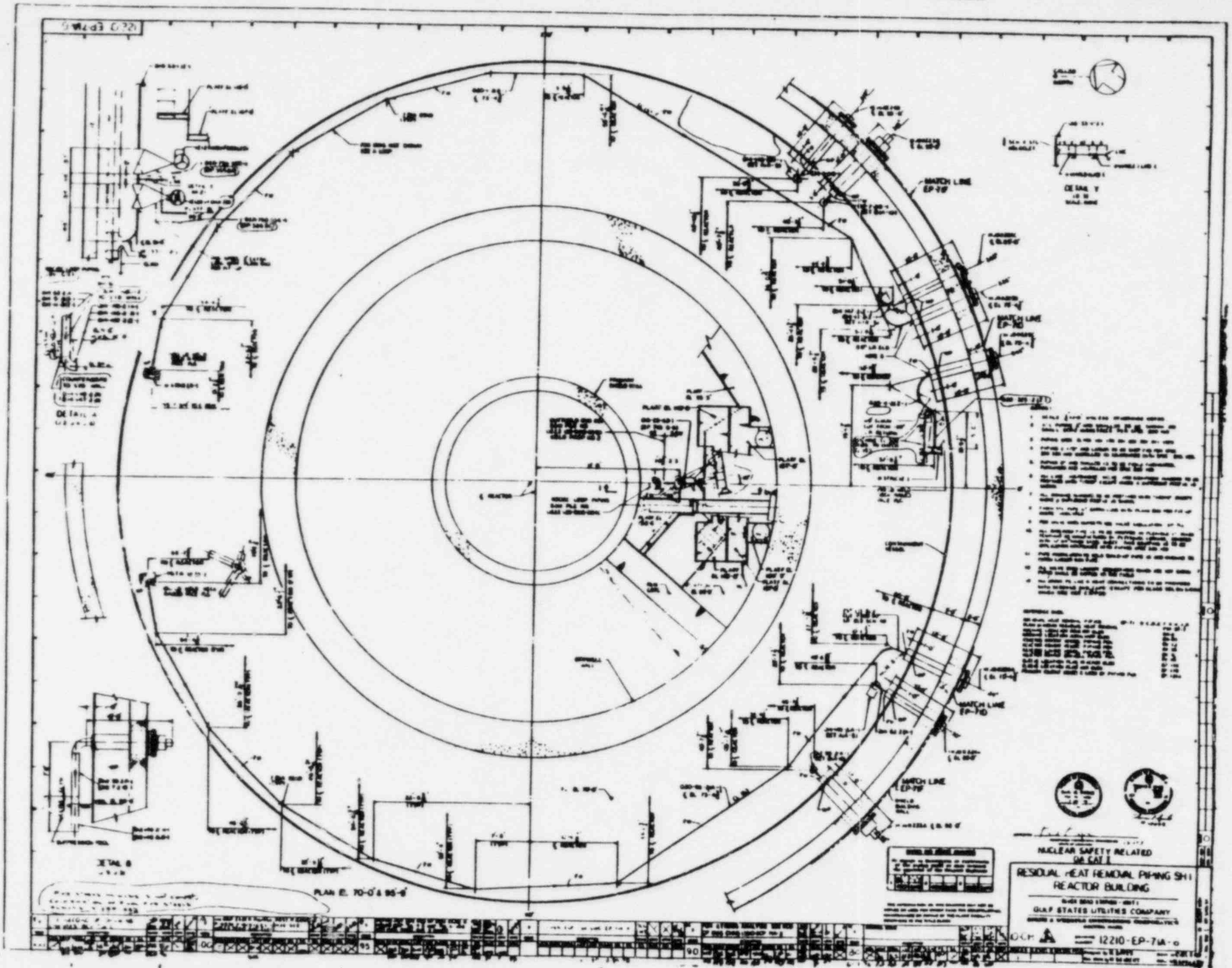
NUCLEAR SAFETY RELATED
QA CAT I
RESIDUAL HEAT REMOVAL PIPING SHT
REACTOR BUILDING
GULF STATES UTILITIES COMPANY
12210-EP-71A-0

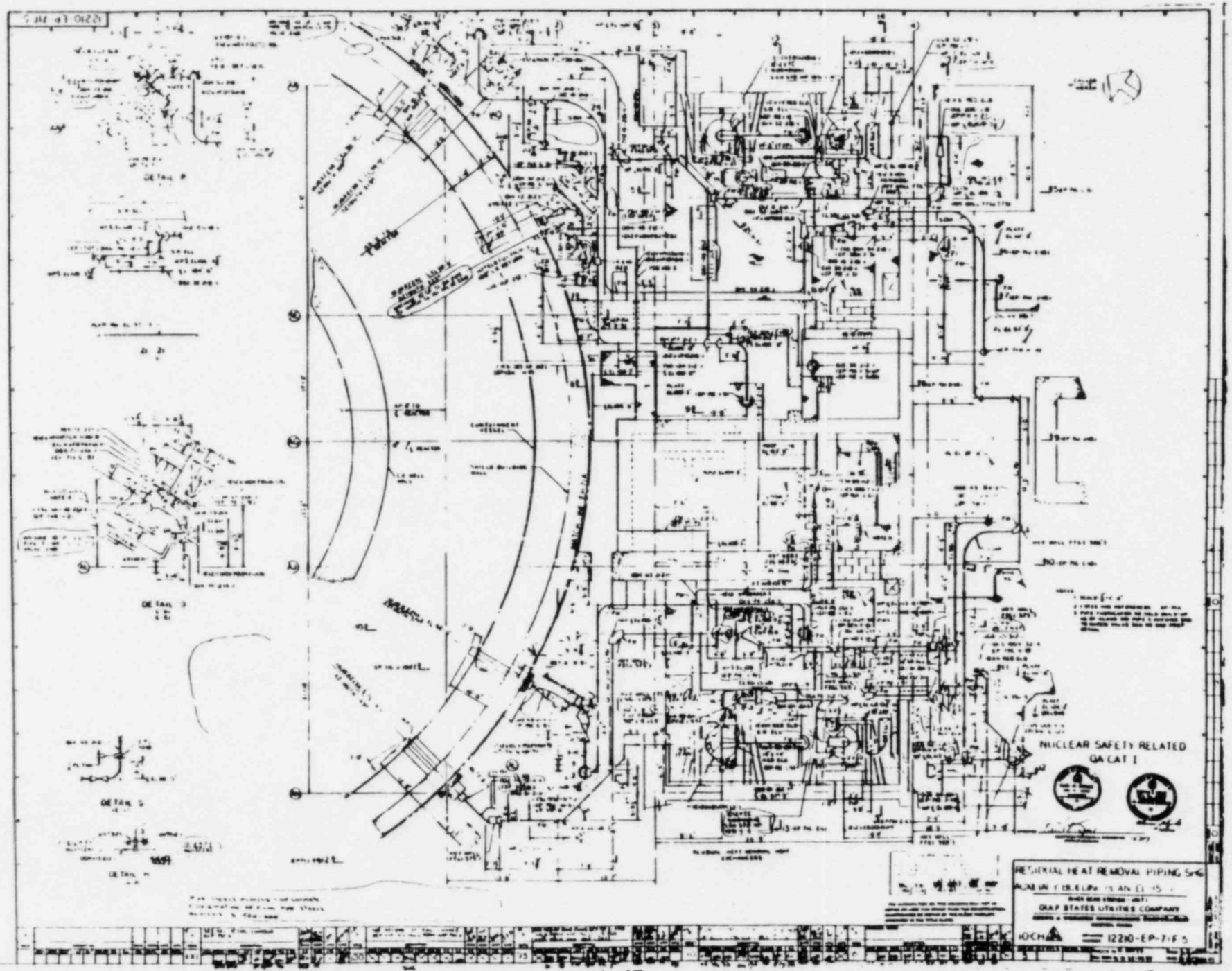
NUCLEAR SAFETY RELATED
QA CAT I
GRAF STATES UTILITIES COMPANY

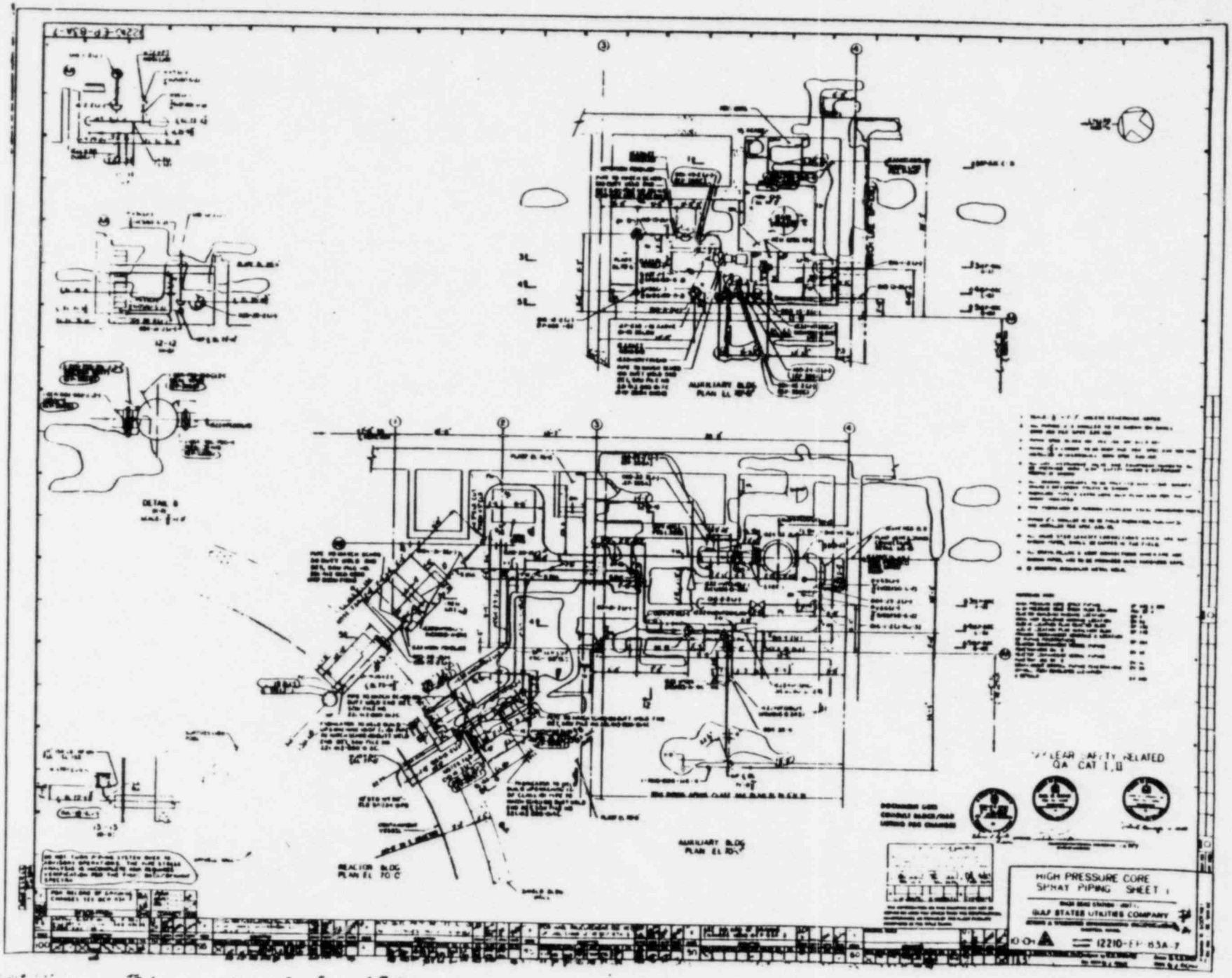
NUCLEAR SAFETY RELATED
QA CAT I,II
HIGH PRESSURE CORE
SPRAY PIPING SHEET 1
GULF STATES UTILITIES COMPANY
12210-EP-85A-7

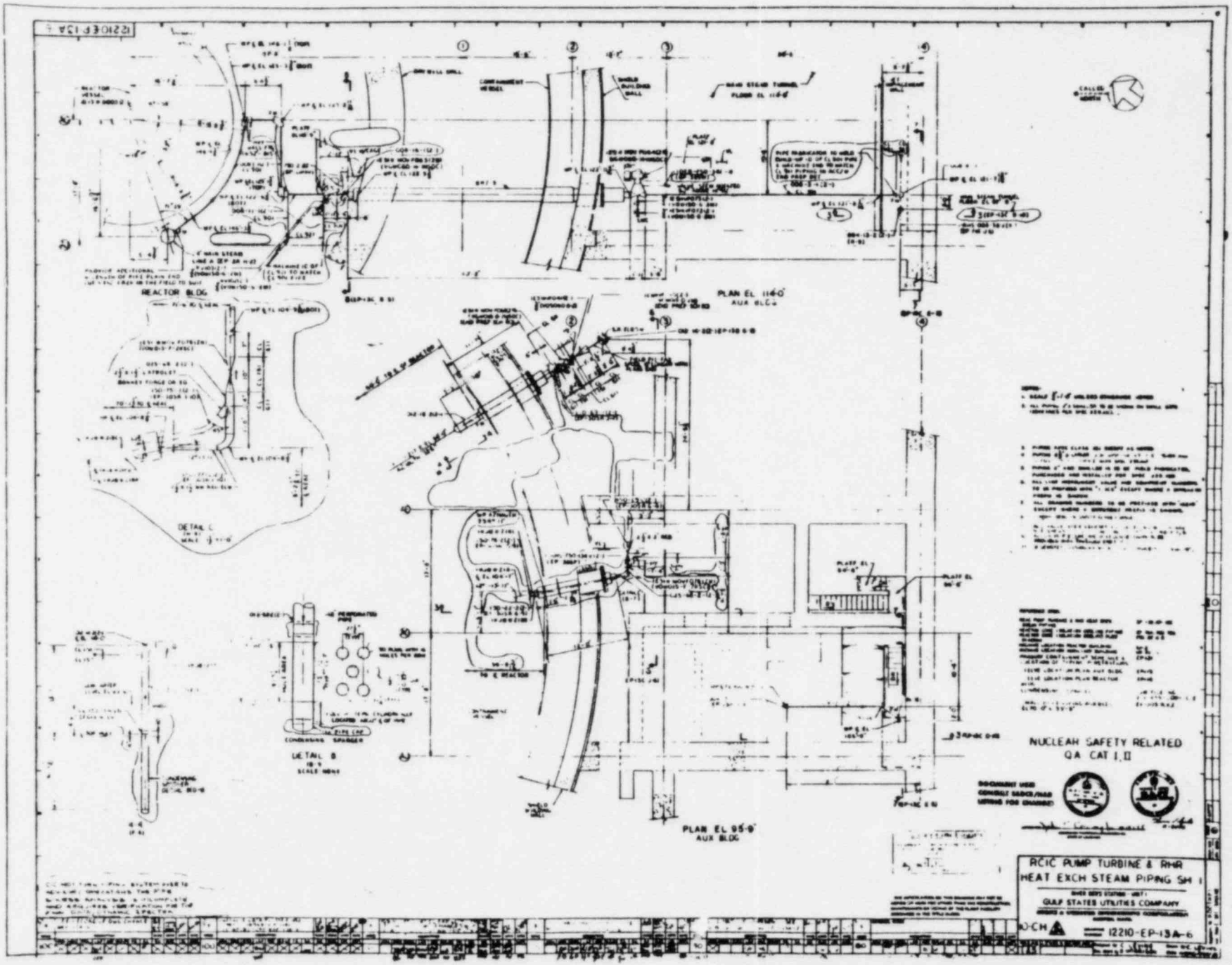
REACTOR BLDG
PLAN EL 114'-0"
AUX BLDG
DETAIL C
DETAIL B
PLAN EL 85'-9"
AUX BLDG
NUCLEAR SAFETY RELATED
QA CAT I, II
RCIC PUMP TURBINE & RHR
HEAT EXCH STEAM PIPING SH 1
GULF STATES UTILITIES COMPANY
12210-EP-13A-6

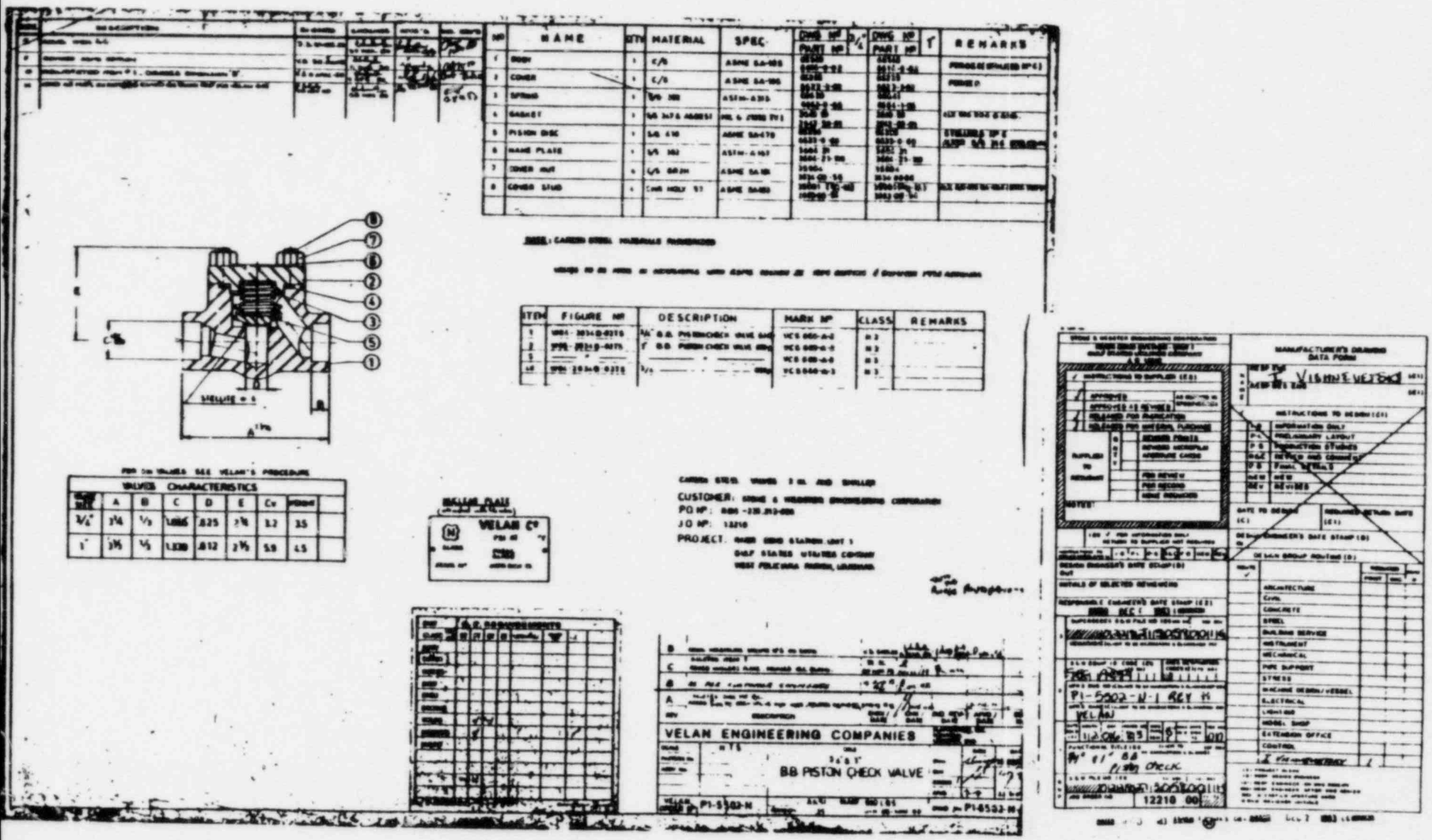

VELAN ENGINEERING COMPANIES

BB PISTON CHECK VALVE

Action Plan 8 - Plant Specific

I. Issues Addressed

3.4 The RHR heat exchanger relief valve discharge lines are provided with vacuum breakers to prevent negative pressure in the lines when discharging steam is condensed in the pool. If the valves experience repeated actuation, the vacuum breaker sizing may not be adequate to prevent drawing slugs of water back through the discharge piping. These slugs of water may apply impact loads to the relief valve or be discharged back into the pool at the next relief valve actuation and apply impact loads to submerged structures.

3.5 The RHR relief valves must be capable of correctly functioning following an upper pool dump, which may increase the suppression pool level as much as 5 ft, creating higher back pressures on the relief valves.

II. Program for Resolution*

1. An analysis will be performed to determine if a water slug from the suppression pool is drawn into the RHR heat exchanger relief valve discharge line.

2. If the analysis shows that water is drawn up from the suppression pool, water slug loads on relief valve piping and submerged structures will be determined and appropriate design modifications implemented if necessary.

3. The River Bend Station design does not incorporate an upper pool dump. Hence, Issue 3.5 is not applicable.

III. Status*

Items 1 through 3 are complete and included with this submittal.

IV. Final Program Results*

A reflood analysis has been performed to determine the water leg rise in the RHR heat exchanger relief valve discharge line, and a subsequent relief valve actuation analysis was performed. The analysis shows that the resulting maximum reflood water elevation is 106.2 ft. The relief valve is at El. 118.75 ft, and there is adequate margin to preclude reflood water from reaching the relief valves. The water clearing loads have been calculated for the relief valve discharge line itself and the adjacent submerged structures. RBS has no structure in the direct jet paths. The induced drag loads affect only a few adjacent structures. Piping and support evaluations for these structures were made, and the structures were found to have sufficient design margin to accommodate these loads. A detailed piping configuration for the RHRHXRVDL for Line A and Line B are shown on Figures 8-1 and 8-2.

The reflood model developed in the Mark I and Mark II program (Reference 1) was used to calculate the water rise in the RHR heat exchanger relief valve discharge line. Following valve closure, the steam/water interface heat transfer coefficient used in the reflood analyses was scaled from vertical vent flow test data (Reference 2). In the vicinity of the pipe exit, a maximum value of heat transfer coefficient was used, considering total bubble collapse. Inside the pipe, the heat transfer coefficient was chosen based on the bubble surface value. The heat transfer coefficient has also been adjusted to account for the influence of the air accumulated from the vacuum breaker near the steam/water interface (References 1 and 3). SWEC computer code STEHAM (FSAR Appendix 3A) was used to calculate dynamic load on piping due to subsequent relief valve actuation. Subsequent actuation was postulated to occur at the maximum reflood level to determine the worst scenario load. The RHR discharge lines have been qualified to these dynamic loads.

Based on this revised response, this issue is considered closed for RBS.

References

1. Wheeler, A. J. and Dougherty, D. A., "Analytical Model for Computing Water Rise in Safety Relief Valve Discharge Line Following Valve Closure," GE Document No. NEDE-23898-P, October 1978

2. Lee, C. K. B. and Chan, C. K., "An Experimental Study of Low Flow Steam Injection Into Subcooled Water, Basic Mechanisms in Two-Phase Flow and Heat Transfer," presented at the ASME Winter Annual Meeting in Chicago, November 16-21, 1980

3. John G. Collier, Convective Boiling and Condensation, McGraw-Hill Book Company (UK) Limited, London 1972

*This revision replaces the GSU submittal dated January 23, 1985

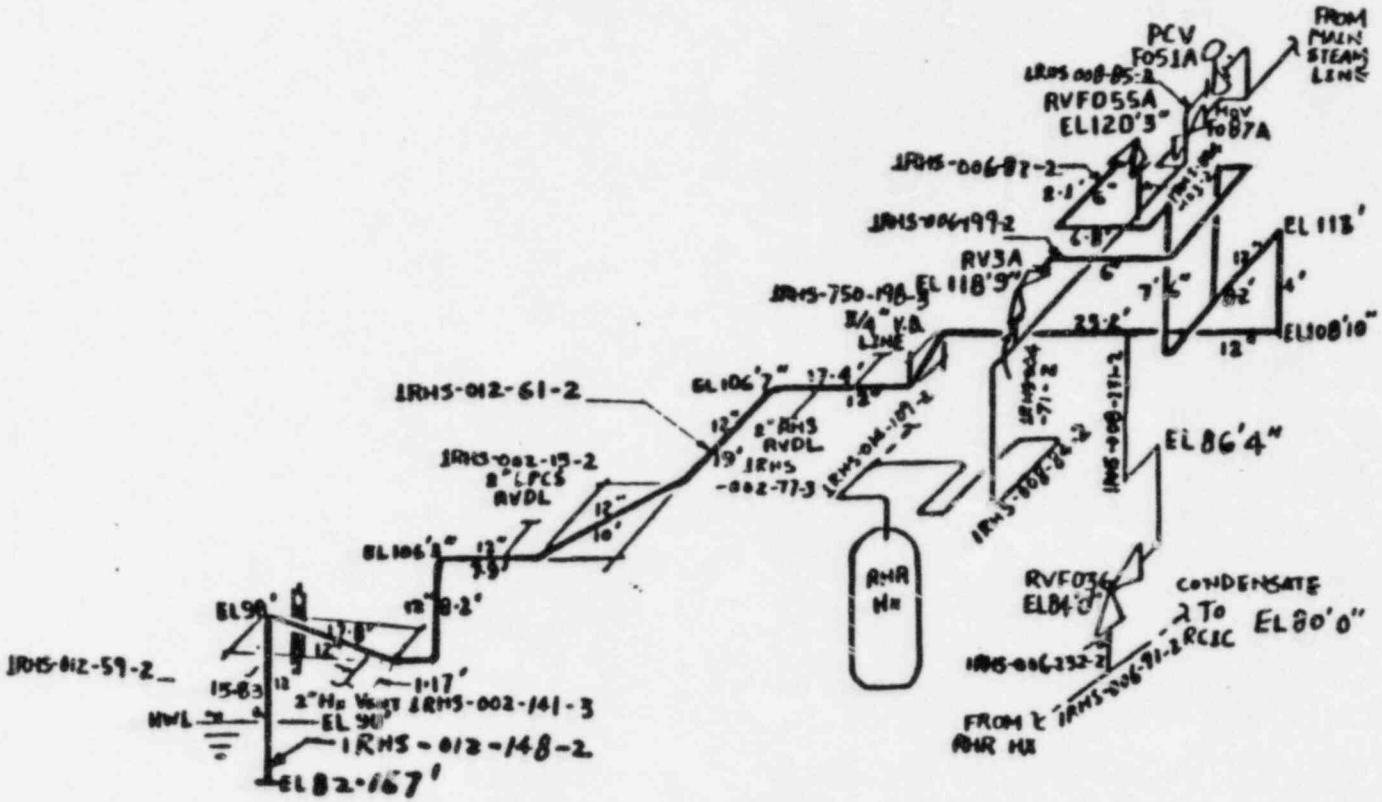

PIPING CONFIGURATION FOR

RHR Hx RELIEF VALVE DISCHARGE

LINE - A FIGURE 8-1

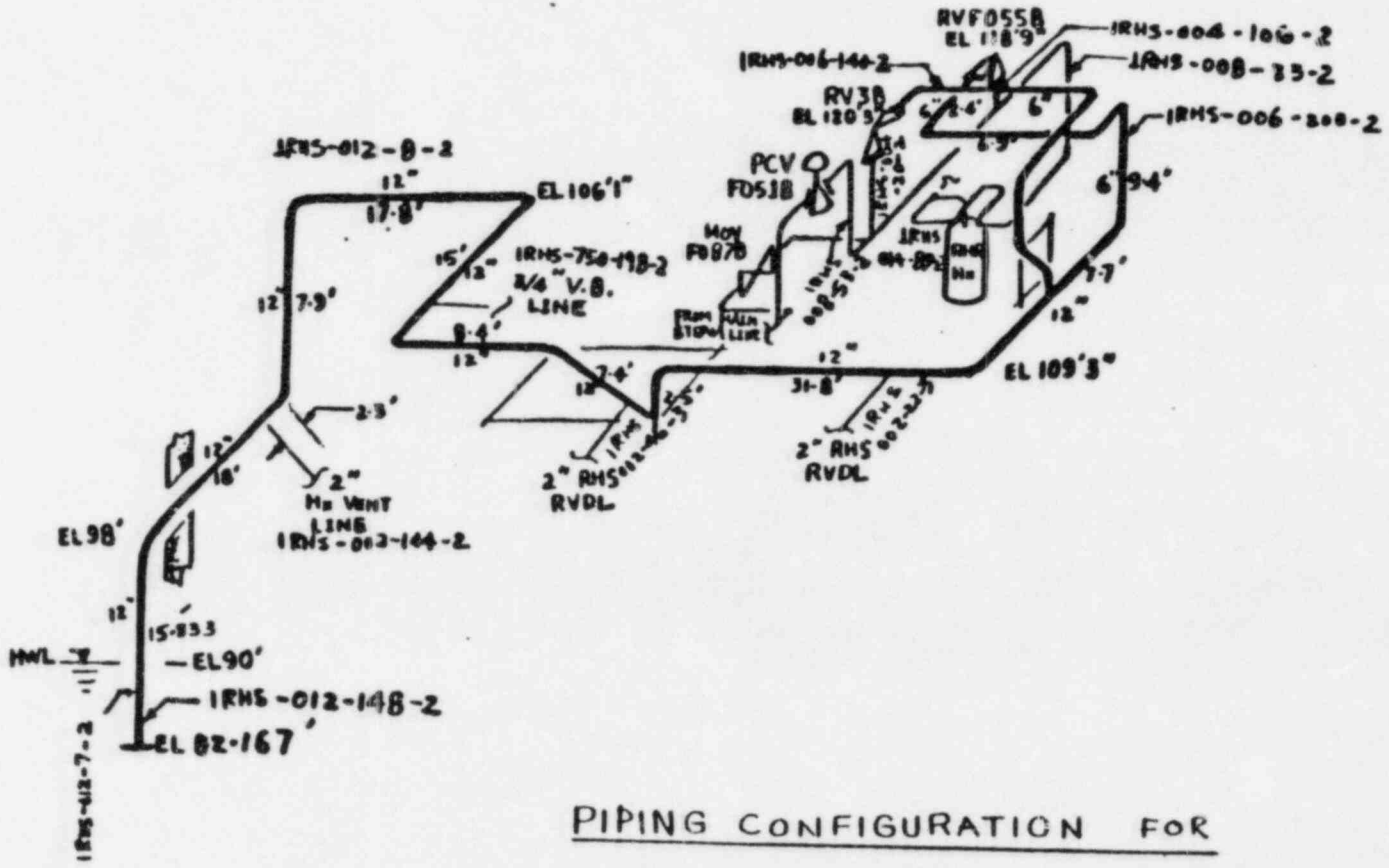

PIPING CONFIGURATION FOR

RHR HX RELIEF VALVE DISCHARGE

LINE-B FIGURE 8-2